

# **Synthesis and Characterization of Mg doped LiMnPO<sub>4</sub> as alternative cathode material for Lithium ion battery**

A dissertation submitted in partial fulfillment of the requirement for the award  
of the degree of

**MASTER OF TECHNOLOGY**

In

**NANO SCIENCE AND TECHNOLOGY**

By

**SNEHA KUMARI**

**(2K16/NST/09)**



Under the Guidance of

**Dr. Amrish K. Panwar**

Assistant Professor

**DEPARTMENT OF APPLIED PHYSICS  
DELHI TECHNOLOGICAL UNIVERSITY  
BAWANA ROAD, DELHI – 110042**

**JULY 2018**

**DEPARTMENT OF APPLIED PHYSICS**  
**DELHI TECHNOLOGICAL UNIVERSITY**  
(Formerly Delhi College of Engineering)  
Bawana Road, Delhi – 110042

**CERTIFICATE**

This is to certify that the dissertation entitled on “**Synthesis and characterization Mg doped LiMnPO<sub>4</sub> as alternative cathode material for Lithium ion battery**” submitted to Delhi Technological University (formerly Delhi College of Engineering) by **Sneha Kumari (2K16/NST/09)** in the partial fulfillment of the requirements for the award of the degree of **Master of Technology in Nano Science and Technology (Applied Physics Department)** is a bona fide record of the candidate's own work carried out under the supervision of **Dr. Amrish K. Panwar**. The information and data enclosed in this thesis is original and has not been submitted elsewhere for honoring any other degree.

**Dr. Amrish K. Panwar**

SUPERVISOR

Assistant Professor

Department of Applied Physics

Delhi Technological University

**Dr. S.C. Sharma**

Head of Department

Department of Applied Physics

Delhi Technological University

**DEPARTMENT OF APPLIED PHYSICS**  
**DELHI TECHNOLOGICAL UNIVERSITY**  
(Formerly Delhi College of Engineering)  
Bawana Road, Delhi - 110042

### **Candidate Declaration**

I hereby declare that the work which is being presented in this thesis entitled “**Synthesis and Characterization of Mg doped LiMnPO<sub>4</sub> as alternative cathode material for Lithium ion battery**” is my own work carried out under the guidance of **Dr. Amrish K. Panwar**, Assistant Professor, Department of Applied Physics, Delhi Technological University, Delhi.

I further declare that the matter embodied in this thesis has not been submitted the award of any other degree or diploma.

Date:

**Sneha Kumari**

Place: New Delhi

**Roll No. -2K16/NST/09**

## **Acknowledgement**

With a great pleasure I would like to express my first and sincere gratitude to my supervisor **Dr. Amrish K. Panwar** for his continuous support, patience, motivating ideas, enthusiasm and immense knowledge. His guidance always enlightens and helped me to shape my work.

Besides my Supervisor, I would like to express my deep gratitude and respect to **Prof. S. C. Sharma**, Head, Department of applied Physics, Delhi Technological University, Delhi for his encouragement, insightful comments and valuable suggestions during the course.

I wish to express my heart full thanks to **Mr. Rakesh Saroha, Mr. Abhishek Bhardwaj** and my friend **Saumya** for their goodwill and support that helped me a lot in successful completion of this project. I also wish to express my heart full thanks to the classmates as well as staff at Department of Applied Physics, Delhi Technological University, Delhi for their goodwill and support that helped me a lot in successful completion of this project.

Finally, I want to thank my parents, brother and friends for always believing in my abilities and for always showering their invaluable love and support.

**Sneha Kumari**

**M. Tech. NST**

**2K16/NST/09**

## **TABLE OF CONTENTS**

SERIAL NO.	TITLE	PAGE NO
1	CERTIFICATE	ii
2	CANDIDATE DECLARATION	iii
3	ACKNOWLEDGEMENT	iv
4	INDEX	6
5	LIST OF FIGURES	8
6	ABSTRACT	10

## **INDEX**

<b>Sr. no.</b>	<b>Title</b>	<b>Page no.</b>
	<b>INTRODUCTION</b>	11
	1.1 History of Lithium ion batteries	11
	1.2 Introduction to Lithium ion batteries	13
	1.2.1 Advantages	14
	1.2.2 Disadvantages	14
	1.3 Methods to improve the performance of lithium ion batteries	15
	1.3.1 Particle size reduction	15
	1.3.2 Composite formation	15
	1.3.3 Doping and functionalization	15
	1.3.4 Morphology Control	16
	1.3.5 Coating and encapsulation	16
	1.3.6 Electrolyte Modification	16
	1.4 Scope of thesis	17
<b>2.</b>	<b>LITERATURE REVIEW</b>	18
	2.1 Development of different type of cathode material	21
	2.1.1 Layered Oxide Cathode	21
	2.1.2 Spinel Oxide Cathode	23
	2.1.3 Polyanion compound- Olivine Structure Cathode	23
	2.2 Various Methods for the synthesis	24
	2.2.1 Solid State reaction	24
	2.2.2 Spray Pyrolysis	25
	2.2.3 Co-Precipitation	25
	2.2.4 Hydrothermal and Solvothermal Routes	25
	2.2.5 Sol gel Synthesis	26
<b>3</b>	<b>SYNTHEIS AND CHARACTERIZATION OF LiMnPO<sub>4</sub></b>	27
	3.1 XRAY diffraction (XRD)	27

	3.2 Scanning electron microscopy (SEM)	29
	3.3 Energy Dispersive Spectroscopy (EDS)	31
	3.4 Synthesis of LiMnPO <sub>4</sub>	32
<b>4</b>	<b>RESULTS AND DISCUSSION</b>	35
	4.1 Characterization results	35
	4.1.1 X-Ray Diffraction Results	35
	4.1.2 Scanning electron microscopy Results	38
	4.1.3 Energy Dispersive spectroscopy Results	42
	4.2 Electrochemical Analysis	45
<b>5</b>	<b>CONCLUSIONS</b>	46
<b>6</b>	<b>REFERENCES</b>	47

## **LIST OF FIGURES**

<b>Sr. No.</b>	<b>Figure Title</b>	<b>Page No.</b>
1.1	Crystal Structure of $\text{LiMnPO}_4$	13
1.2	Typical Lithium ion battery showing the motion of $\text{Li}^+$ ion from anode to cathode and vice-versa	14
1.3	Various methods to improve the performance of $\text{LiMnPO}_4$	17
2.1	Crystal Structure of $\text{LiCoO}_2$ (Layered Structure)	22
2.2	Crystal Structure of $\text{LiMn}_2\text{O}_4$ (Spinel Structure)	23
2.3	Crystal Structure of $\text{LiFePO}_4$ (Olivine Structure)	24
3.1	Front view of XRD	28
3.2	Bragg's Law	29
3.3	Schematic of Scanning electron microscopy	31
3.4	Flow chart for the synthesis of $\text{LiMnPO}_4$ (LMP), $\text{LiMn}_{0.99}\text{Mg}_{0.01}\text{PO}_4$ (LMMP1) and $\text{LiMn}_{0.97}\text{Mg}_{0.03}\text{PO}_4$ (LMMP3)	32
4.1	XRD result of $\text{LiMnPO}_4$ prepared using $300^\circ\text{C}$ and $600^\circ\text{C}$ for 12 hrs by solid state reaction method	36
4.2	XRD result of $\text{LiMn}_{0.99}\text{Mg}_{0.01}\text{PO}_4$ prepared using $300^\circ\text{C}$ and $600^\circ\text{C}$ for 12 hrs by solid state reaction method	37
4.3	XRD result of $\text{LiMn}_{0.97}\text{Mg}_{0.03}\text{PO}_4$ prepared at $300^\circ\text{C}$ and $600^\circ\text{C}$ for 12 hrs by solid state reaction method	37
4.4	SEM images of $\text{LiMnPO}_4$ at 5x and 10x zoom	39
4.5	SEM images of $\text{LiMn}_{0.99}\text{Mg}_{0.01}\text{PO}_4$ at 5x and 10x zoom	40
4.6	SEM images of $\text{LiMn}_{0.97}\text{Mg}_{0.03}\text{PO}_4$ at 5x and 10x zoom	41
4.7	EDS image of $\text{LiMnPO}_4$	42
4.8	Composition of $\text{LiMnPO}_4$	42
4.9	EDS image of $\text{LiMn}_{0.99}\text{Mg}_{0.01}\text{PO}_4$	43
4.10	Composition of $\text{LiMn}_{0.99}\text{Mg}_{0.01}\text{PO}_4$	43



4.11	EDS image of $\text{LiMn}_{0.97}\text{Mg}_{0.03}\text{PO}_4$	44
4.12	Composition of $\text{LiMn}_{0.97}\text{Mg}_{0.03}\text{PO}_4$	44

## **ABSTRACT**

The pristine  $\text{LiMnPO}_4/\text{C}$  (LMP/C) and Mg-doped  $\text{LiMn}_{0.99}\text{Mg}_{0.01}\text{PO}_4$  (LMMP1) and  $\text{LiMn}_{0.97}\text{Mg}_{0.03}\text{PO}_4$  (LMMP3) samples have been synthesized for cathode material. In this study, the pristine and Mg doped  $\text{LiMnPO}_4$  cathode material is prepared using solid state route. Physicochemical characterization of the synthesized materials has been performed using X-ray diffraction (XRD), Scanning electron microscope (SEM) and Energy dispersive spectroscopy (EDS) to confirm proper phase formation, particle size and determination of composition respectively. The XRD patterns reveal the formation of the pure phase orthorhombic olivine structure of the pristine  $\text{LiMnPO}_4/\text{C}$  (LMP/C) and Mg-doped  $\text{LiMn}_{0.99}\text{Mg}_{0.01}\text{PO}_4$  and  $\text{LiMn}_{0.97}\text{Mg}_{0.03}\text{PO}_4$  samples with Pnmb space group. SEM micrographs show the formation of dispersed, nanosized particle for the synthesized samples. Electrochemical performances for this pristine and Mg doped  $\text{LiMnPO}_4$  are further analyzed.

# CHAPTER 1

## INTRODUCTION

### 1.1 HISTORY OF Li-ION BATTERIES:

Li-ion batteries are ordinate of high energy, high power density and long cyclebility energy devices, which makes them useful for various applications such as hybrid electric vehicles, portable electronics, and power tools [1]. Li-ion may be alternate to reduce green house gas emission, as the gasoline powered transportation are being replaced by the electric vehicles powered by lithium ion batteries. The high energy efficiency of Li-ion batteries can be utilized in numerous applications such as electrical grid, and storage of electric energy extracted from renewable energy resources such as solar, wind, tidal and geo-thermal etc. The Li-ion batteries have various advantages compared to other commercial batteries. Li-ion batteries have the highest cell potential as Li is known to have the lowest reduction potential among all elements in the periodic table. It has the smallest ionic radii, since it is the third lightest element. Due to these factors, Li-ion batteries have high volumetric capacity and power density. Although multivalent cations allow them for higher charge capacity per ion, but the additional charge reduces their mobility [2].

Nowadays,  $\text{LiCoO}_2$  is well known commercialized cathode material in Li-ion batteries. But due to toxic and hazardous nature, it is unsafe and also expensive. Therefore, developing a cathode material, environment friendly, thermally stable and cost effective cathode material.  $\text{LiCoO}_2$  has been replaced by other spinel and olivine type cathode materials [3].

Compared to various commercially employed cathode materials based on  $\text{LiCoO}_2$  or  $\text{LiNiO}_2$  (layered structure), manganese based  $\text{LiMn}_2\text{O}_4$  (spinel structure), and olivine-type lithium transition metal phosphates  $\text{LiMPO}_4$  where  $\text{M} = \text{Fe}, \text{Mn}, \text{Co}, \text{Ni}$  are considered to be more efficient cathode materials for lithium ion batteries as their properties gets improved because of doping [4].

In past few years,  $\text{LiFePO}_4$  has attracted more attention because of its high performance in terms of energy demands, power density and cyclability, high theoretical capacity. In Olivine  $\text{LiMnPO}_4$ , the materials with  $M = \text{Mn, Co, Ni}$  can offer much higher potentials as compared to  $\text{LiFePO}_4$ . Olivine structured  $\text{LiFePO}_4$  is much demanding cathode material in lithium ion batteries, because of its environmental friendliness, low toxicity low cost, high thermal stability and high specific capacity.  $\text{LiMnPO}_4$  is known to have same theoretical capacity as of  $\text{LiFePO}_4$  viz 170mAh/g, but as it higher potential of 4.1 V compared to  $\text{LiFePO}_4$ , therefore it is best known cathode material which can be used in place of  $\text{LiFePO}_4$  which have only 3.4 V potential [5]. It delivers higher energy density. This Olivine type material has 3-D structure which comprises of strong covalent bonds between  $\text{P}^{5+}$  and oxygen ions forming  $\text{PO}_4^{3-}$  tetrahedral polyanions [1]. Therefore during lithiation and de-lithiation olivine metal phosphate doesn't undergo a structural re-arrangement. This means that the capacity do not degrade during cycling process which is the problem faced by lithium transition metal oxides structure of cathodes such as  $\text{LiCoO}_2$   $\text{LiNiO}_2$ ,  $\text{LiMnO}_2$  and  $\text{LiMn}_2\text{O}_4$ . However,  $\text{LiMnPO}_4$  shows slow  $\text{Li}^+$  ion diffusion and have very low electronic conductivity, which leads to its poor electrochemical performance. Due to Poor electrochemical performance, the applications of  $\text{LiMnPO}_4$  have certain drawbacks. There are two major factors which deteriorate the electrochemical performance of  $\text{LiMnPO}_4$  extremely low ionic and electronic conductivity and the structural instability during the electrochemical process. Over the few decades, the poor conductivity in  $\text{LiMnPO}_4$  has been improved using carbon coating or ion doping or substitution. However, the structural issue has not been undertaken much attention in the past. Due to the asymmetric electronic configuration of  $\text{Mn}^{3+}$  ions in  $\text{LiMnPO}_4$ , it faces lattice deformation in the charged  $\text{LiMn}^{\text{II}}\text{PO}_4$  phase. Due to this large lattice misfit along with the Jahn-teller deformation between  $\text{LiMnPO}_4$  and  $\text{MnPO}_4$  phases effects the lattice structure, leading to low electrochemical performance. But several methods such as metal cation doping, morphology controlling, carbon coating and particle reducing have improved the electrochemical performance of  $\text{LiMnPO}_4$  [6].

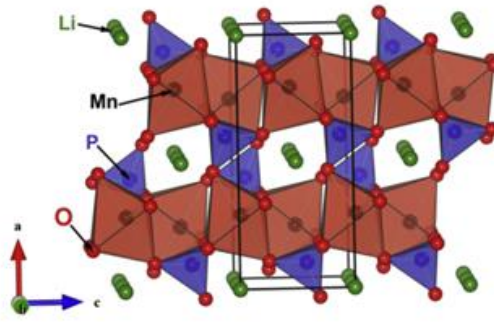


Fig 1.1 Crystal Structure of  $\text{LiMnPO}_4$  [7]

## 1.2 INTRODUCTION TO Li-ION BATTERIES:

Lithium ion battery is one kind of the rechargeable batteries which consists of positive electrode called cathode and negative electrode called electrode. In lithium ion batteries, lithium ions moves from the anode to cathode during discharge and back when charging. An intercalated lithium compounds has been used as the host electrode material instead of metallic lithium used in the non-rechargeable batteries where the guest ions of Li ions gets accumulated and removed repeatedly while charging and discharging action. The metallic lithium electrode material increases the dendrite formation leading to thermal runaway in rechargeable batteries and consequently it results in the explosion of the rechargeable batteries. Hence to overcome this problem, lithium is intermixed with the lithium based compound such as  $\text{LiFePO}_4$ ,  $\text{LiCoO}_2$ ,  $\text{LiMn}_2\text{O}_4$ ,  $\text{LiMnPO}_4$  etc. Usually Lithium ion batteries consist of functional components which are as follows:

- Anode –Used as negative electrode made of C/SnSb or low discharge potentials
- Cathode- Used as positive electrode- it consists mainly of metal oxides
- Electrolyte – It is made of non-aqueous liquid of lithium like  $\text{LiPF}_6$ ,  $\text{LiBF}_4$ ,  $\text{LiClO}_4$  etc.
- Separator – It is made of insulating materials which has property to pass through  $\text{Li}^+$  ions and prevent electron conduction in battery.

During discharge, current flows from the anode to the cathode due to lithium ions  $\text{Li}^+$ , through the non- aqueous electrolyte, where the guest ions of lithium flow back to the host. During charging, a higher potential but of the same polarity is applied through a external power supply than that produced by the battery forcing the current to flow in the reverse direction and while charging guest lithium ions from the intercalated host cathode material flow from cathode to anode. The lithium ions then flows from cathode to the anode where they get accumulated in the porous electrode material and this process known as intercalation [7].

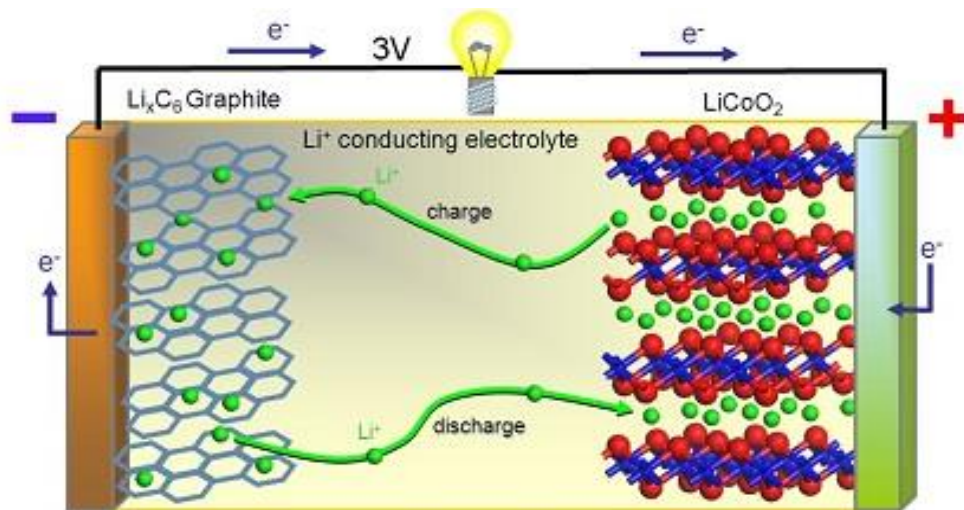


Fig 1.2 Typical Lithium ion battery showing the motion of  $\text{Li}^+$  ion from anode to cathode and vice-versa

### 1.2.1 ADVANTAGES:

- Higher power
- Higher voltage
- Light weight

### 1.2.2 DISADVANTAGES:

- Expensive
- Delicate – Battery temperature should be monitored from inside it should be sealed properly.

- Toxic – Shipping Li-ion battery in bulk is risky. It is a hazardous material and thus it increases its price while shipping.

### **1.3 METHODS TO IMPROVE THE ELECTROCHEMICAL PERFORMANCE OF LiMnPO<sub>4</sub>:**

There are various methods to improve the electrochemical performance of LiMnPO<sub>4</sub> cathodes. Some of them are as follows:

1. Particle size reduction
2. Composite formation
3. Doping and functionalization
4. Morphology control
5. Coating and encapsulation
6. Electrolyte Modification

#### **1.3.1 PARTICLE SIZE REDUCTION:**

It has been seen that by reducing the particle size the Li<sup>+</sup> ions diffusion path is effectively shortened and the large interfacial area for electrochemical reaction is provided by high surface area which is obtained by reducing the size, thus leading to excellent rate performance and high discharge capacity. It makes ion and electron transport faster. Therefore on reducing particle size, stress(s) are relieved and it also improves the mechanical stability [7].

#### **1.3.2 COMPOSITE FORMATION:**

Composite formation provides conductive media for electrons in the cathode material. It also provides mechanical and structural support [7].

#### **1.3.3 DOPING AND FUNCTIONALIZATION:**

It has been seen that doping LiMnPO<sub>4</sub> may improve the electronic conductivity and structural compatibility on the electrochemical process. It is observed that some ions such as

$\text{Mg}^{2+}$ ,  $\text{Fe}^{2+}$ ,  $\text{Ni}^{2+}$ , and  $\text{Cu}^{2+}$  showed a positive effect on electrochemical performance whereas on doping or substitution  $\text{Zn}^{2+}$  and  $\text{Ti}^{4+}$  indicate the negative effect. There are some impurities present in the Zn and Ti substituted sample which influences the activity of the material and thus mask the effect of Zn and Ti substitution [5][7].

#### 1.3.4 MORPHOLOGY CONTROL:

Morphology control provides improvement in structural stability as well as modified reactivity. It also promotes faster ion, electron and phonon transport [7].

#### 1.3.5 COATING AND ENCAPSULATION:

Coating the cathode material gives protection from electrolyte and also provides protection of the electrolyte decomposition. It also helps in stabilization of surface reactions. It provides a conductive media to the cathode material [7].

#### 1.3.6 ELECTROLYTE MODIFICATION:

Formation of passivation layer(s) on the the surface of cathode material is due to the modification in the electrolyte. It also helps in controlled solubility of active material(s) and decomposition product(s) [7].



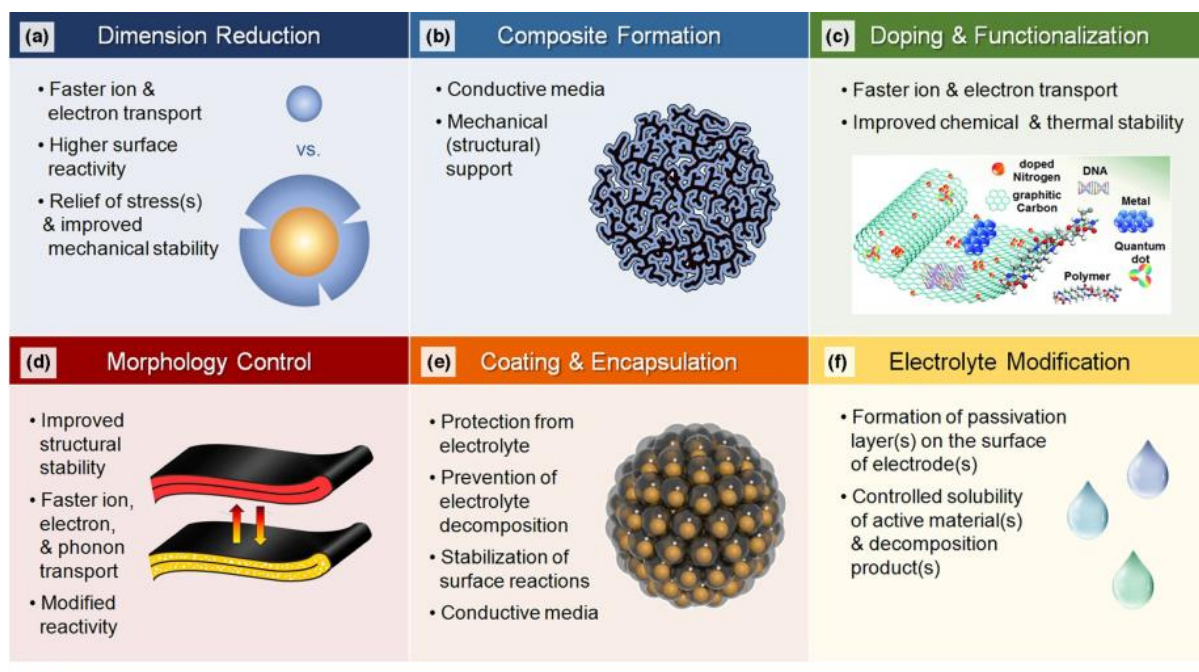


Fig 1.3 showing various ways for improving the performance of  $\text{LiMnPO}_4$  [7]

## 1.4 SCOPE OF THESIS:

The work done here in this thesis depicts the synthesis and characterization of Mg doped  $\text{LiMnPO}_4/\text{C}$  as the alternative cathode material for lithium ion batteries using solid state reaction route. The characterization includes X-ray diffraction (XRD), Scanning electron microscopy (SEM) and Energy dispersive spectroscopy (EDS) of bare  $\text{LiMnPO}_4$ , 1% and 3% Mg doped with  $\text{LiMnPO}_4$ .

## CHAPTER 2

### LITERATURE REVIEW

In the recent work, Qiao Ying Huang used Solid state reaction route as synthesis route, and prepared  $\text{LiMnPO}_4/\text{C}$ ,  $\text{LiMn}_{0.85}\text{Fe}_{0.15}\text{PO}_4/\text{C}$ ,  $\text{LiMn}_{0.92}\text{Ti}_{0.08}\text{PO}_4/\text{C}$  and  $\text{Li}(\text{Mn}_{0.85}\text{Fe}_{0.15})_{0.92}\text{Ti}_{0.08}\text{PO}_4/\text{C}$ . He then characterized these samples using (XRD), X-Ray photoelectron spectroscopy(XPS), SEM and electrochemical tests. There was considerable amount of enhancement with the co-doping of  $\text{Ti}^{4+}$  and  $\text{Fe}^{2+}$  at the Mn sites which lead to performance improvement of  $\text{LiMnPO}_4$  and improvement in lithium ion diffusion. Among these two co-dopant  $\text{Li}(\text{Mn}_{0.85}\text{Fe}_{0.15})_{0.92}\text{Ti}_{0.08}\text{PO}_4/\text{C}$  showed better rate capability and higher discharge capacity [5].

Haisheng Fang synthesized  $\text{LiMn}_{0.8}\text{Fe}_{0.19}\text{Mg}_{0.01}\text{PO}_4/\text{C}$  using solid state reaction route and then characterized by (XRD), (SEM) and electrochemical test.  $\text{LiMn}_{0.8}\text{Fe}_{0.19}\text{Mg}_{0.01}\text{PO}_4/\text{C}$  was carbon coated with 8 wt. %, with size approximately in the range of 100-500nm and aggregated into microparticles around 3-5 $\mu\text{m}$ . Inspite of less carbon coating and larger size, the electrochemical test showed the good cyclability and high capacity of  $\text{LiMn}_{0.8}\text{Fe}_{0.19}\text{Mg}_{0.01}\text{PO}_4/\text{C}$  [8].

Haisheng Fang showed that 2 wt % of Zn is useful for the performance of  $\text{LiMnPO}_4$  because of the reduced charge transfer resistance. This doping lead to the increased lithium ion diffusion and phase conversion.  $\text{LiMn}_{0.98}\text{Zn}_{0.02}\text{PO}_4$  has better rate capability and much higher capacity as compared to the  $\text{LiMnPO}_4$  [9].

Ling Wu prepared  $\text{LiMnPO}_4$  using sol-gel combined with ball milling and liquid nitrogen quenching method. It was understood from XRD results that the structure of  $\text{LiMnPO}_4$  was not destroyed by quenching. The quenched sample showed the much contracted lattice parameters as compared to the unquenched sample. SEM results showed that the agglomeration of  $\text{LiMnPO}_4/\text{C}$  particles was controlled using nitrogen quenching. The numbers of defects were formed in the crystal of  $\text{LiMnPO}_4$  which was justified using TEM results. The quenched samples showed much higher discharge capacities as those compared with un-quenched ones [3].

Wenxuan Zhang synthesized  $\text{LiMnPO}_4$  nanoplates by a facile solvothermal in mixed water DEG (diethylene glycol) with mediation of CTAB (cetyltrimethyl ammonium bromide). The crystal orientation of  $\text{LiMnPO}_4$  was along the ac plane due to the coordinative effect of CTAB and DEG. The size of these nanoplates were of about 13nm. The characterization of the  $\text{LiMnPO}_4$  was done using XRD, SEM, FTIR and Raman Spectra. The  $\text{LiMnPO}_4$  was uniformly carbon coated after the treatment with sucrose. The given sample showed high discharge capacity and high performance [4].

Jingmin fan prepared  $\text{LiMnPO}_4$  through a facile two step method. While the synthesis process the Oleylamine was introduced as solvent and the carbon source. The  $\text{LiMnPO}_4$  particle has the size approximately about 40 nm with the carbon coating of 2-3nm. The prepared  $\text{LiMnPO}_4$  material showed higher discharge capacity. The carbon coating improves the electronic and the ionic conductivity and the cycling ability of the sample was also stabilized [1].

Thierry Drezen prepared  $\text{LiMnPO}_4$  via sol-gel method. After subjecting the sample at different temperature between 520-600°C, the particle size obtained was in the range of 140-220 nm. Further dry ball milling reduced the size of the particle from 130-90nm. The better electrochemical performance and higher charging rates were observed when smaller  $\text{LiMnPO}_4$  particles were used [6].

Zhijian Zhang prepared  $\text{LiMnPO}_4$  with the surface co-coating of  $\text{Li}_2\text{TiO}_3$  along with the carbon coating by quasi sol-gel after the thermal treatment. The Characterization was the sample was done using XRD, SEM, EDS, TEM, XPS, TEM, XPS. The  $\text{Li}_2\text{TiO}_3$ - coated  $\text{LiMnPO}_4$  illustrated better lithium ion diffusion and higher cycle stability as compared to the  $\text{LiMnPO}_4$ . The best electrochemical performance results were obtained when the 3 wt %  $\text{LiTiO}_3$  coated  $\text{LiMnPO}_4$  sample [10].

Zhumabay bakenov prepared  $\text{LiMnPO}_4$  via spray pyrolysis along with the wet ball milling by utilizing different conductive carbon which are acetylene black and the other types of ketjen black. The ketjen black preferred as compared with other conductive carbon since larger surface area. Material with these coating shows large discharge capacity compared with other  $\text{LiMnPO}_4$ . By using these conductive carbons, the charge transfer and lithium ion transport was improved [11].

Nam Long Doan combined Spray pyrolysis and wet ball milling followed by heat treatment for the method of preparation  $\text{LiMnPO}_4$ . Spray pyrolysis had the heat treatment range in  $200\text{--}500^\circ\text{C}$ . XRD detected that there was no impurity phase in the sample. The size of the sample was determined using scanning electron microscopy and transmission electron microscopy with size approximately in the range of 100nm. The sample synthesized with the temperature range of  $300^\circ\text{C}$  using spray pyrolysis gave the best electrochemical performance because of the smaller particle size, larger specific surface area and carbon coating [12].

Jiangfeng Ni prepared  $\text{LiMnPO}_4$  using high energy ball milling. The characterization of the sample were done using XRD, SEM, Raman spectroscopy, Laser particle analysis and galvanostatic charge discharge. The  $\text{LiMnPO}_4$  material synthesized using acetylene black provided better electrochemical performance than those compared without using acetylene black [2].

Nicholas P.W Pieczonka compared the method of preparation of  $\text{LiMnPO}_4$  by polyol and solid state reaction method for lithium ion batteries. The characterization of the sample was done using XRay and neutron powder diffraction, SEM, TEM and electrochemical characterization. The same amount of Li/Mn cation mixing was done which is about 4-5%. The flower-like morphology of  $\text{LiMnPO}_4$  whose growth rate was in the direction parallel to bc plane was obtained using polyol method. The carbon sources were Shawinigan acetylene black and super P black for carbon coating. The  $\text{LiMnPO}_4$  prepared using super P black has better cathode performance as compared to that of Shawinigan acetylene black [13].

Zhong Sheng Kui prepared  $\text{LiMnPO}_4$  using sol-gel method by adding citric acid. The characterization of the sample was done using XRD, SEM and electrochemical performance. The XRD results shows the sample prepared at low temperature of  $500^\circ\text{C}$ , the olivine structure of  $\text{LiMnPO}_4$ . The SEM results showed that the citric acid controlled the particle size of  $\text{LiMnPO}_4$  because of the presence of citric acid. This method leads to high electrochemical performance of  $\text{LiMnPO}_4$  [14].

Fang Wen synthesized  $\text{LiMnPO}_4$  by facile assisted solvothermal route. The  $\text{LiMnPO}_4$  particles thus prepared were of size 3-10nm. Thus the mesoporous  $\text{LiMnPO}_4$  nanoparticles

showed high discharge capacity, high electrochemical performance for cathode materials for lithium ion batteries. These mesoporous  $\text{LiMnPO}_4$  improves ionic and electronic transport [15].

Manickam Minakshi prepared  $\text{LiMnPO}_4$  via sucrose induced combustion method with Co and Ni as co-dopant. The sample thus prepared was hence tested in aqueous based LiOH electrolyte. The changes were observed during the characterization in the lattice parameters and peak positions. The Ni and Co in  $\text{LiMnPO}_4$  induced Jahn Teller  $\text{Mn}^{3+}$  ions distortion. Hence the discharge capacity was highly enhanced.  $\text{LiMn}_{0.5}\text{Co}_{0.5}\text{PO}_4$  and  $\text{LiMn}_{0.33}\text{Co}_{0.33}\text{Ni}_{0.33}\text{PO}_4$  were smaller size which reduced the electron transport length. The cell voltage was improved with extended cell capacity and good capacity [16].

## **2.1 DEVELOPMENT OF DIFFERENT TYPE OF CATHODE**

### **MATERIALS:**

The solid host network of  $\text{LiMnPO}_4$  intercalated cathode material stores guest ions. The guest ions can be inserted and can be removed from the host network repeatedly. In Lithium ion battery,  $\text{Li}^+$  ions are the guest ions and the host is the intercalated transition metal oxides. These cathode materials are divided into various categories according to their crystal structures such as layered, spinel, Olivine and tavorite. These crystal structure were developed to produce high energy density, high capacity, high power density, high capacity, long cyclic life, light weight, low self discharge, environment friendly and cost effective of lithium ion batteries. Among these various type of developed cathode olivine type  $\text{LiMnPO}_4$  is one of the prospect for high discharge voltage and thereby good power density. Detailed investigation of these cathodes is as follows [7]. In this investigation, olivine type  $\text{LiMnPO}_4$  structure of cathode material has been studied.

#### **2.1.1 LAYERED OXIDE CATHODE:**

The Co and Li are placed in the octahedral positions which occupy alternating layers to form hexagon symmetry. Due to its high theoretical capacity of 274mAh/g, high theoretical

volumetric capacity of 1363 mAh/cm<sup>3</sup>, therefore it has gained a lot of attention commercially. It also exhibits properties like low self discharge, high discharge voltage. But its poor low thermal stability leads to exothermic reaction. When these cathode materials are heated above a certain point, the heat is released along with the oxygen and hence it is not a perfect option to use it at high temperature. Moreover, deep cycling generally refers to delithiation above 4.1 V by distorting the lattice structure from hexagonal to monoclinic symmetry and this change reduces the cycling performance. Hence, different types of other transition metals (Mn, Al, Fe, Cr) were examined as possible substitutes for Co. In order to improve the LCo stability and performance even during deep cycling. The coating of various metal oxides such as Al<sub>2</sub>O<sub>3</sub>, B<sub>2</sub>O<sub>3</sub>, TiO<sub>2</sub>, ZrO<sub>2</sub> were attempted to keep structure stability at high temperature. LiNiO<sub>2</sub> (LNO) also have the same layered crystal structure as LiCoO<sub>2</sub>. It is comparatively cheaper and also have high energy density as compared to LiCoO<sub>2</sub>. During synthesis and delithiation, the Ni<sup>2+</sup> ions replace the Li<sup>+</sup> sites by blocking the path of Li<sup>+</sup> ions diffusion, therefore, pure LNO cathode may not be a ordinate cathode materials. Since Ni<sup>3+</sup> can reduced as compared to Co<sup>3+</sup>, therefore LNO has more thermal stability. Hence, the issue of low thermal stability has been resolved by adding small amount of Al, and Mg to improve the thermal stability and electrochemical performance of LCO. Since Mn is much cheaper and less toxic as compared to Co or Ni, LiMnO<sub>2</sub> has also been considered as promising cathode material in lithium ion batteries. During the lithium ion extraction, layered structure may change to spinel structure, therefore the cycling performance of LMO is poor [7].

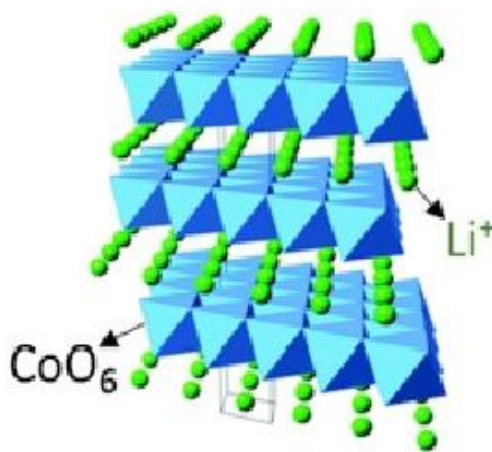


Fig 2.1 Crystal Structure of LiCoO<sub>2</sub> (Layered structure)

### 2.1.2 SPINEL OXIDE CATHODE:

Spinel  $\text{LiMn}_2\text{O}_4$  is available abundant, cost effective and environment friendly. Li is placed tetrahedral sites and Mn is at octahedral sites. In the 3-D,  $\text{Li}^+$  ions can diffuse into vacant tetrahedral and octahedral interstitial sites. It has poor long term cyclability because of the Jahn teller distortion in  $\text{Mn}^{3+}$  ions and it has side reaction with electrolyte, leading to oxygen loss from the delithiated  $\text{LiMn}_2\text{O}_4$ . By reducing the size to nanoparticles, the rate performance may be considerably improved because of shorter  $\text{Li}^+$  diffusion lengths and improved electronic transport [7].

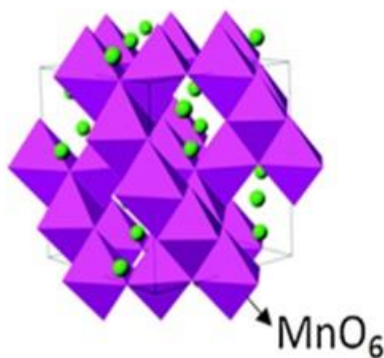


Fig 2.2 Crystal Structure of  $\text{LiMn}_2\text{O}_4$  (Spinel structure)

### 2.1.3 OLIVINE STRUCTURE CATHODE - POLYANION COMPOUND:

Polyanion are placed at lattice positions and increases cathode redox potential.  $\text{LiFePO}_4$  (LFP) represents the Olivine structure due its thermal stability and high power capabilities. In LFP,  $\text{Li}^+$  and  $\text{Fe}^{2+}$  are placed at octahedral sites while P is at tetrahedral sites in a slightly distorted hexagonal closely packed oxygen array. The major drawbacks of  $\text{LiFePO}_4$  are low average potential, electrical and ionic conductivity. With effective cationic doping, carbon coating and particle size reduction, the rate performance can be improved. If particles are uniformly nanosized and conductive nanocarbon is used inside the cathode material, thus

improving the electrochemical performance without carbon coating.  $\text{LiMnPO}_4$  offers 0.4 V higher average voltage, which contributes higher specific energy but its conductivity is low [7].

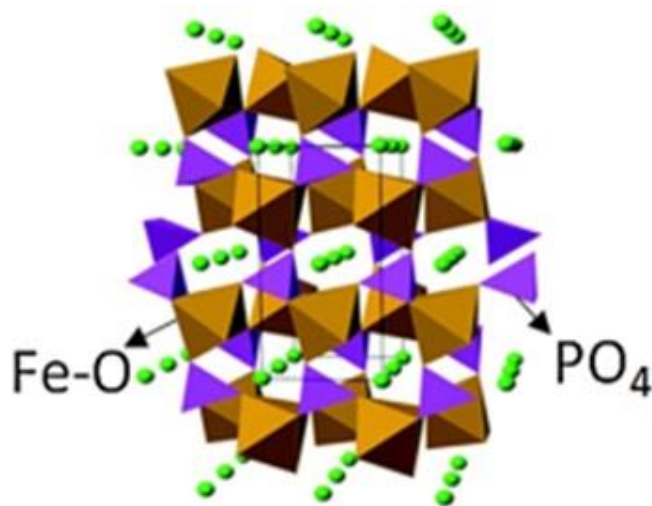


Fig 2.3 Crystal Structure of  $\text{LiFePO}_4$  (Olivine structure)

## 2.2 VARIOUS METHODS FOR THE SYNTHESIS/TECHNIQUE:

There are several synthesis methods have been used to synthesis the desired cathode materials. Among these some of the common techniques/methods of synthesis are given as:

1. Solid state reaction
2. Spray pyrolysis
3. Co-precipitation
4. Hydrothermal and Solvothermal Routes
5. Sol gel Synthesis

### 2.2.1 SOLID STATE REACTION:

The solid state reaction is the conventional method of synthesis which requires two-step heating treatment, in which first heating temperature range is  $300^\circ\text{C}$  -  $400^\circ\text{C}$  and another of the range of  $600^\circ\text{C}$  or more. As it is simple and easy for making large amount of product, therefore it is used for mass production of the method. The use of high temperature increases the cost of



technology, and the other drawback that as the temperature is very high which leads to agglomeration of particles, thus the product produced is not of small size (particularly in nano range). Therefore it is advised to add carbon and use of lesser temperature while processing the product [17].

### 2.2.2 SPRAY PYROLYSIS:

Spray Pyrolysis is the method used for the preparation of ultrafine particles. The principal underlying it is to obtain the ultrafine particle by the generation of droplets in a continuous way from a solution containing precursor of colloidal particles. Methods like ultrasonic transduction leads to the formation of these droplets. For the generation of droplets acts as the nucleation centers and then become dense and crystallizes and thus forming pure particles in the spray pyrolysis method. The product thus formed is collected in a series of water bubblers at the reactor outlet where the salt by product dissolves and thus leaving desired material behind [17].

### 2.2.3 CO-PRECIPITATION:

Co-precipitation method has utilizes lower temperature as compared to the solid state reaction method. It is also known for lesser reaction time. The particle size can be reduced up to the nanometer level and this reduction in size helps to improve the charge-discharge capacity especially in the large current condition. The problem arises while the complex process of mass production and it consumes a lot power [17].

### 2.2.4 HYDROTHERMAL AND SOLVOTHERMAL ROUTES:

Hydrothermal and solvothermal synthesis is a chemical process. In this process occurs in aqueous solution of mixed precursors above the boiling temperature of water and alcohol respectively. In this method, calculation steps can be avoided and thus obtain the pure powder directly from the heated solution. It is necessary to carry out the calcinations step at high temperatures for carbon coating. During this synthesis, heated alcohol or water accelerates the diffusion of particles and crystal growth is comparatively fast. Both routes are carried out in a

closed system called autoclave and there are less environmental concerns than any another technology [17].

#### 2.2.5 SOL-GEL:

Sol gel synthesis is also a low temperature chemical process as compared to solid state reaction method. It is used for the preparation of metal oxides. Sol-gel synthesis comprises the formation of a sol. The sol is a stable colloidal suspension of solid particles in a solvent. The gelation of this sol forms a gel which have pores made of colloidal particles. The cross linking ratio and the particle size determines the properties of gel. The gel is then dried to form xerogel, which shows reduced volume. All liquid is removed from the surface of the pores by using high temperature to obtain the final product, which also reduces the number and connectivity of pores. Reaction parameters such as time, pH, temperature, precursor, concentration, viscosity, solvent, etc are important for the formation of like shape, particle size, porosity, pore size, morphology and distribution of particle in the obtained powder. The surface of the powder product is controlled from the beginning of the reaction in the sol gel synthesis. Sol gel synthesis uses lower temperature and therefore it is low cost. Advantages of this method are precise stoichiometry, high purity of the sample obtained, its uniform structure and very small size [17].

# **CHAPTER 3**

## **SYNTHESIS**

### **AND CHARACTERIZATION OF $\text{LiMnPO}_4$**

The work in this dissertation involves the synthesis of pristine  $\text{LiMnPO}_4$ , and  $\text{LiMnPO}_4$  doped with wt. 1% and wt. 3%, thus forming  $\text{LiMn}_{0.99}\text{Mg}_{0.01}\text{PO}_4$  and  $\text{LiMn}_{0.97}\text{Mg}_{0.03}\text{PO}_4$  respectively. The theoretical capacity of  $\text{LiMnPO}_4$  is about 170 mAh/g and average potential is 4.1 V, but its electronic and ionic conductivity is low as compared to other olivine type materials. In order to its electrochemical performance and electronic conductivity, the pristine  $\text{LiMnPO}_4$  is doped with Mg which shows positive effect in improving its discharge capacity and electrochemical performance. The method of preparation of  $\text{LiMnPO}_4$ ,  $\text{LiMn}_{0.99}\text{Mg}_{0.01}\text{PO}_4$  and  $\text{LiMn}_{0.97}\text{Mg}_{0.03}\text{PO}_4$  are solid state reaction routes, which involves two step heating process. In the first heating step, the temperature used is in the range of 300° C - 400° C and in another heating step, the temperature used is in the range of 600°C or more. This method is used for the mass production of the material. The cost of technology increases due to the high temperature utilized. Due to the high temperature there is agglomeration of particles, therefore the material thus produced cannot be of small size (particularly in nano range). The methods like adding carbon and using lesser temperature can be used while processing the material.

#### **3.1 X-RAY DIFFRACTION (XRD):**

The atomic and molecular structure of the crystal can be determined using XRD method. In this method, the beam of incident X-Ray is diffracted in specific direction by the crystalline atoms. By measuring the angles and intensities of these diffracted beams, the 3-D image of the density of electron inside the crystal can be determined. Any crystallographic disorder, their chemical bond, their positions inside the atoms and other information inside the crystal can also be found out.



Fig 3.1 Front view of XRD

Scattering phenomenon is also known as diffraction. The atoms at the lattice sites scatter incident beam in all possible directions when the beam of X-ray strikes the crystalline structure. The different set of planes in crystalline structure acts as diffraction gratings. The wavelength of the X-Ray and for a particular set of planes in certain direction and gives the strong beam. The diffracted beam has much weaker intensity as compared to the incident beam or the transmitted beam. The diffracted beam is composed of large number of scattered rays. Diffraction differ with reflection in many ways such as diffracted beam is built up of rays scattered by all the atoms of the crystal which lie in path of incident beam. It occurs only at those angles which satisfy bragg's law. The intensity is very small as compared to incident beam whereas Reflection takes place in a thin surface layer only. It can occurs any angle of incidence and it is 100% efficient with good mirror. The angle between diffracted and transmitted beam which is  $2\theta$  is known as diffraction

angle. The wavelength of this diffracted beam can be found using given formal, which is,  $\lambda = 2d\sin\theta$ .

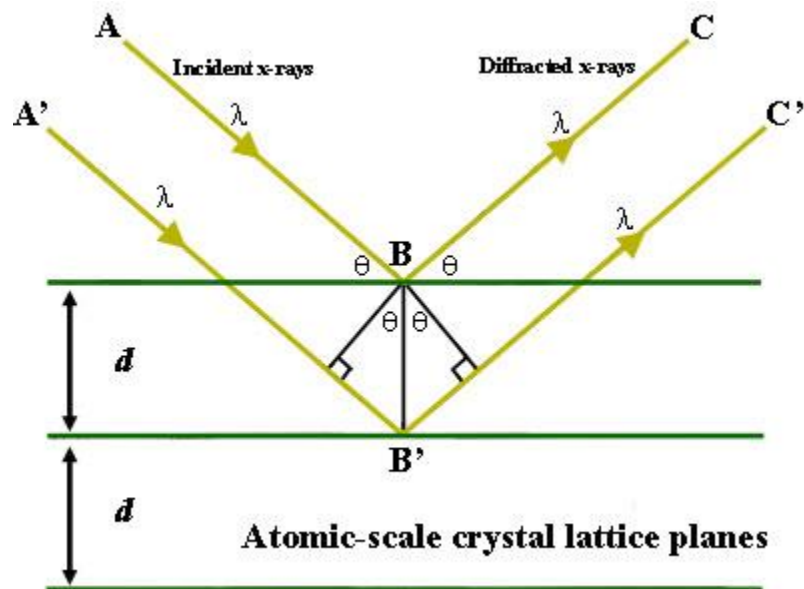


Fig 3.2 depicting the bragg's law

### 3.2 SCANNING ELECTRON MICROSCOPE (SEM):

A Electron microscopy also known as SEM, in which by focusing with the beam of electrons, an image of sample is produced. The image thus produced contains the information about the sample such as the size of the particles, composition of the sample. Image is produced when the electrons interacts with the atoms inside the sample. A source of electron is focused through the vacuum and with the help of fine probe it is rastered over the surface of the sample, so as to give the information about the sample. The electron beam are deflected horizontally and vertically when it is passed through the scan coils and objective lens so as to scan the sample. When the electrons interacts with the atoms within the sample, it results in the emission of electrons or photons from the surface of the sample. Detectors are utilized to collect the electrons emitted. These collected electrons are then used to modulate the output signal of cathode ray tube while rastering over the surface of the sample. Thus an image is produced by focusing the beam

of electrons on the sample and observed on the CRT where the magnification is  $M=L/l$  where,  $L$  is raster length of CRT monitor and  $l$  is the raster length on surface of sample. The SEM voltage is approximately 2-50 KV and the beam diameter is 5nm-2 $\mu$ m.

The principle images produced in SEM are three types:

- Secondary electron images – Secondary electron images are produced when energy of emitted electron is less than 50 eV. The secondary electrons are emitted due inelastic scattering. When the beam of electrons is focused on the sample, transfer of energy can be observed. The beam of electrons which is focused on the surface of the sample is known as primary electrons and the electrons which are then emitted from the surface of the sample is known as secondary electrons. These secondary electrons are then detected by positive bias collector or detector. The energies of the primary electrons determine the quantity of secondary electrons emitted from the sample. The emission of secondary electrons is dependant on the energy of the primary electrons. The energies of secondary electrons is limited to 50 eV.
- Backscattered electron images – The energy of electrons emitted from the sample is greater than 500eV. Electrons exit the specimen with energy greater than 500 eV. The backscattered electrons are emitted due to elastic scattering. Images formed due to backscattered electrons have poor resolution than those formed due to secondary electrons since the energy is obtained from the much deeper location within the sample. The backscattered electrons have definite direction and have energy more than 2KeV. The backscattered electrons are emitted due to the primary electrons. To distinguish between different type of samples, backscattered electrons are used. The backscattered electrons cannot be collected using secondary electrons detectors.

The SEM may be equipped with EDS (Energy distributed X-Ray spectrum) for obtaining the compositional details of the sample. EDS is helpful in obtaining the contaminants present in the sample. It is also helpful in estimating in the concentration of the sample.

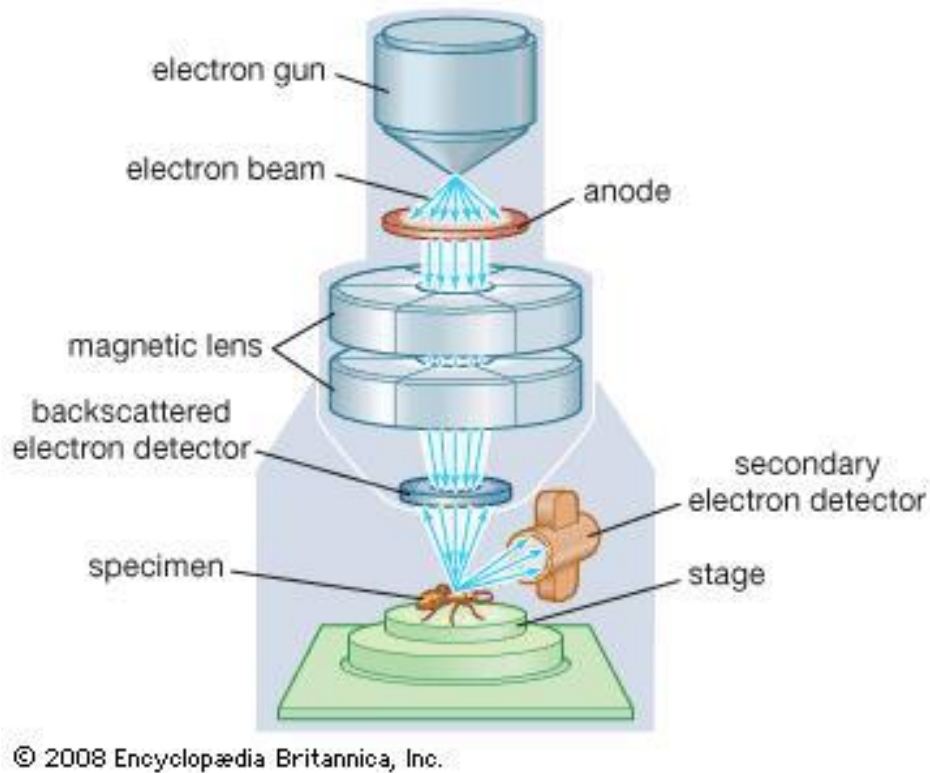


Fig 3.3 Schematic of Scanning electron microscopy

### 3.3 ENERGY DISPERSIVE SPECTROSCOPY (EDS):

Scanning electron microscopy is also equipped Energy dispersive spectroscopy which is used for obtaining the compositional details of the sample. The characteristics X-rays interact with the sample which is produced by the high energy. The energy and intensities of the characteristics X- Ray are compared with one another for finding compositional details of the sample under analysis.

### 3.4 SYNTHESIS OF $\text{LiMnPO}_4$ :

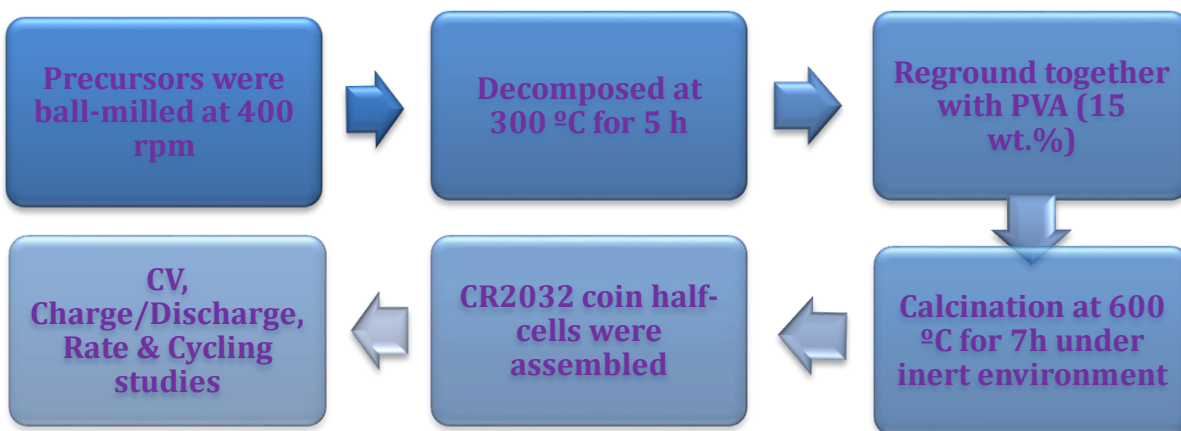


Fig 3.4 Flow chart for the synthesis of  $\text{LiMnPO}_4$  (LMP),  $\text{LiMn}_{0.99}\text{Mg}_{0.01}\text{PO}_4$  (LMMP1) and  $\text{LiMn}_{0.97}\text{Mg}_{0.03}\text{PO}_4$  (LMMP3)

The  $\text{LiMnPO}_4$  (LMP) material was prepared via a solid state reaction route with starting materials of  $\text{LiOH}\cdot\text{H}_2\text{O}$  (99%, purity),  $\text{MnO}$  (99%, purity) and  $\text{NH}_4\text{HPO}_4$  (99%, purity). Stoichiometric amount of raw materials was weighed. For improving the electrochemical performance of pristine  $\text{LiMnPO}_4$  (LMP) it is doped with Mg in place of Mn with 1% and 3% by weight, as  $\text{LiMn}_{0.99}\text{Mg}_{0.01}\text{PO}_4$  (LMMP1) and  $\text{LiMn}_{0.97}\text{Mg}_{0.03}\text{PO}_4$  (LMMP3) respectively.  $\text{LiMn}_{0.99}\text{Mg}_{0.01}\text{PO}_4$  and  $\text{LiMn}_{0.97}\text{Mg}_{0.03}\text{PO}_4$  was prepared by solid state reaction route where the basic chemicals used are  $\text{LiOH}\cdot\text{H}_2\text{O}$  (99%, purity),  $\text{MnO}$  (99%, purity) and  $\text{NH}_4\text{HPO}_4$  (99%, purity),  $\text{Mg}(\text{CH}_3\text{COO})_2$  (99%, purity). The precursors were put into a stainless steel vessel for ball milling with stainless steel balls keeping reactants ball mass ratio of 20:1. The container and contents were then subjected to high energy ball milling. The duration of this milling was kept



12 hrs at 400 rpm for all the samples of LMP, LMMP1 and LMMP3. The milled powder was collected. The mixture was first dried in oven at 60° C for 24 hr. The mixture was decomposed at 300°C for 5 hr, in the presence of Ar. The sample was mixed with 15% of polyvinyl alcohol (PVA) and ball milled for another 3 hr. Then the sample is decomposed at again 600° C for 7 hr in the presence of Ar atmosphere.

#### LiMnPO<sub>4</sub>:

Following steps were followed in the preparation:

1. Lithium hydroxide monohydrate,  $\text{LiOH} \cdot \text{H}_2\text{O} = 41.96 \times (99\% \text{ purity}) = 41.5404 \text{ gmol}^{-1}$
2. Manganese Oxide,  $\text{MnO} = 70.94 \times (99\% \text{ purity}) = 70.2306 \text{ gmol}^{-1}$
3. Ammonium phosphate dibasic,  $(\text{NH}_4)_2\text{HPO}_4 = 132.06 \times (99\% \text{ purity}) = 130.7394 \text{ gmol}^{-1}$

$$\text{Total mass} = 41.5404 + 70.2306 + 130.7394 = 242.5104 \text{ gmol}^{-1}$$

The Ball weight to sample ratio was taken as 20:1.

$$\text{So, Li} = (41.5404/242.5104) \times 7.806 = 1.3371 \text{ gm}$$

$$\text{Mn} = (70.2306/242.5104) \times 7.806 = 2.2606 \text{ gm}$$

$$\text{PO}_4 = (130.7394/242.5104) \times 7.806 = 4.208 \text{ gm}$$

$$\text{Total weight} = 1.3371 + 2.2606 + 4.208 = 7.8059 \text{ gm}$$

#### LiMn<sub>0.99</sub>Mg<sub>0.01</sub>PO<sub>4</sub> (1% wt.):

Following steps were followed in the preparation:

1. Lithium hydroxide monohydrate,  $\text{LiOH} \cdot \text{H}_2\text{O} = 41.96 \times (99\% \text{ purity}) = 41.5404 \text{ gmol}^{-1}$
2. Manganese Oxide,  $\text{MnO} = 70.94 \times (99\% \text{ purity}) = 70.2306 \text{ gmol}^{-1}$   
 $1 \text{ mole} = 70.2306 \text{ gm}$   
 $0.99 \text{ mole} = 0.99 \times 70.2306 = 69.5282 \text{ gmol}^{-1}$
3. Ammonium phosphate dibasic,  $(\text{NH}_4)_2\text{HPO}_4 = 132.06 \times (99\% \text{ purity}) = 130.7394 \text{ gmol}^{-1}$
4. Magnesium acetate tetra hydrate,  $(\text{Mg}(\text{CH}_3\text{COO})_2) = 214.45 \times (99\% \text{ purity}) = 212.3055 \text{ gmol}^{-1}$

$$1 \text{ mole} = 212.3055 \text{ gm}$$

$$0.01 \text{ mole} = 212.3055 \times 0.01 = 2.1230 \text{ gmol}^{-1}$$

$$\text{Total mass} = 41.5404 + 69.5282 + 130.7394 + 2.1230 = 243.931 \text{ gmol}^{-1}$$

The Ball weight to sample ratio was taken as 20:1.

$$\text{So, Li} = (41.5404/243.93)*7.806 = 1.3293 \text{ gm}$$

$$\text{Mn} = (69.5282/243.93)*7.806 = 2.2474 \text{ gm}$$

$$\text{PO}_4 = (130.7394/243.93)*7.806 = 4.1837 \text{ gm}$$

$$\text{Mg} = (2.1230/243.931)*7.806 = 0.0679 \text{ gm}$$

$$\text{Total weight} = 1.3371+2.2474+4.1837+0.0679 = 7.8059 \text{ gm}$$

LiMn<sub>0.97</sub>Mg<sub>0.03</sub>PO<sub>4</sub> (3% wt.):

Following steps were followed in the preparation:

1. Lithium hydroxide monohydrate, LiOH.H<sub>2</sub>O = 41.96\*(99% purity) = 41.5404 gmol<sup>-1</sup>

2. Manganese Oxide, MnO = 70.94\*(99% purity) = 70.2306 gmol<sup>-1</sup>

$$1 \text{ mole} = 70.2306 \text{ gm}$$

$$0.97 \text{ mole} = 0.97* 70.2306 = 68.123 \text{ gmol}^{-1}$$

3. Ammonium phosphate dibasic, (NH<sub>4</sub>)<sub>2</sub>HPO<sub>4</sub> = 132.06\*(99% purity) = 130.7394 gmol<sup>-1</sup>

4. Magnesium acetate tetra hydrate, (Mg(CH<sub>3</sub>COO)<sub>2</sub>) = 214.45\*(99% purity) = 212.3055 gmol<sup>-1</sup>

$$1 \text{ mole} = 212.3055 \text{ gm}$$

$$0.03 \text{ mole} = 212.3055*0.03 = 6.3691 \text{ gmol}^{-1}$$

$$\text{Total mass} = 41.5404+68.123+130.7394+6.3691 = 246.7719 \text{ gmol}^{-1}$$

The Ball weight to sample ratio was taken as 20:1.

$$\text{So, Li} = (41.5404/246.7719)*7.806 = 1.3140 \text{ gm}$$

$$\text{Mn} = (68.123/246.7719)*7.806 = 2.1548 \text{ gm}$$

$$\text{PO}_4 = (130.7394/246.7719)*7.806 = 4.135 \text{ gm}$$

$$\text{Mg} = (6.3691/246.7719)*7.806 = 0.2014 \text{ gm}$$

$$\text{Total weight} = 1.3140+2.1548+4.135+0.2014 = 7.8059 \text{ gm}$$

## CHAPTER 4

### RESULT AND DISCUSSION

#### 4.1 CHARACTERIZATION RESULTS:

##### 4.1.1 X-RAY DIFFRACTION:

The atomic and molecular structure of the crystal can be determined using XRD method. In this method, the beam of incident X-Ray is diffracted in specific direction by the crystalline atoms. By measuring the angles and intensities of these diffracted beams, the 3-D image of the density of electron inside the crystal can be determined. Any crystallographic disorder, their chemical bond, their positions inside the atoms and other information inside the crystal can also be found out.

In this work XRD results were used to determine crystal structure and morphology of the samples produced. The X-ray diffraction have utilized Cu-K $\alpha$  radiation ( $k = 1.5406 \text{ \AA}$ ) between  $10^\circ$ - $90^\circ$ . Powder X-ray diffraction (XRD) analysis was carried out to determine the composition and structure of the  $\text{LiMnPO}_4$ ,  $\text{LiMn}_{0.99}\text{Mg}_{0.01}\text{PO}_4$  and  $\text{LiMn}_{0.97}\text{Mg}_{0.03}\text{PO}_4$ . All the peaks are indexed to a pure orthorhombic olivine structure of  $\text{LiMnPO}_4$  (LMP),  $\text{LiMn}_{0.99}\text{Mg}_{0.01}\text{PO}_4$  (LMMP1), and  $\text{LiMn}_{0.97}\text{Mg}_{0.03}\text{PO}_4$  (LMMP3) with a Pnmb space group. The high peak intensities suggest the high crystallinity of  $\text{LiMnPO}_4$ ,  $\text{LiMn}_{0.99}\text{Mg}_{0.01}\text{PO}_4$  and  $\text{LiMn}_{0.97}\text{Mg}_{0.03}\text{PO}_4$  powders. The main peaks at  $2\theta = 16.92^\circ$ ,  $22.45^\circ$ ,  $25.31^\circ$ ,  $29.24^\circ$ ,  $35.193^\circ$ ,  $52.42^\circ$  and  $61.121^\circ$  are indication of proper  $\text{LiMnPO}_4$ ,  $\text{LiMn}_{0.99}\text{Mg}_{0.01}\text{PO}_4$  and  $\text{LiMn}_{0.97}\text{Mg}_{0.03}\text{PO}_4$  phases. No diffraction peaks associated with impurities noticed. The formation of  $\text{LiMnPO}_4$  phase would be helpful for the electrons and ions transport  $\text{LiMnPO}_4$  material during electrochemical analysis. From FWHM crystallite size of LMP, LMMP1 and LMMP3 has been estimated from the observed XRD data and it is found that the crystallite/particle size calculated using scherrer formula for LMP is  $1.084 \times 10^{-12}$ , for LMMP3 it is  $8.93 \times 10^{-13}$  which shows that the size is decreasing after doping of Mg in place of Mn. The particle size reduction could shorten the  $\text{Li}^+$

diffusion pathway, which would improve the electrochemical performance of the  $\text{LiMnPO}_4$  cathode material.

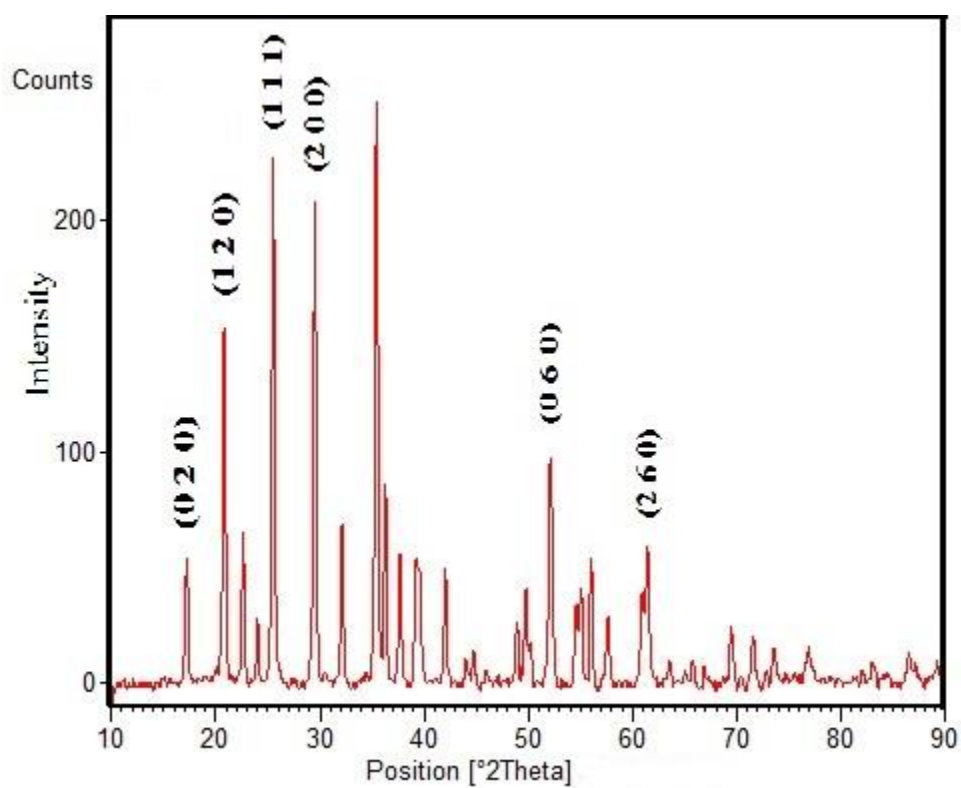


Fig 4.1 XRD result of  $\text{LiMnPO}_4$  prepared using 300 $^{\circ}\text{C}$  and 600 $^{\circ}\text{C}$  for 12 hrs by solid state reaction method

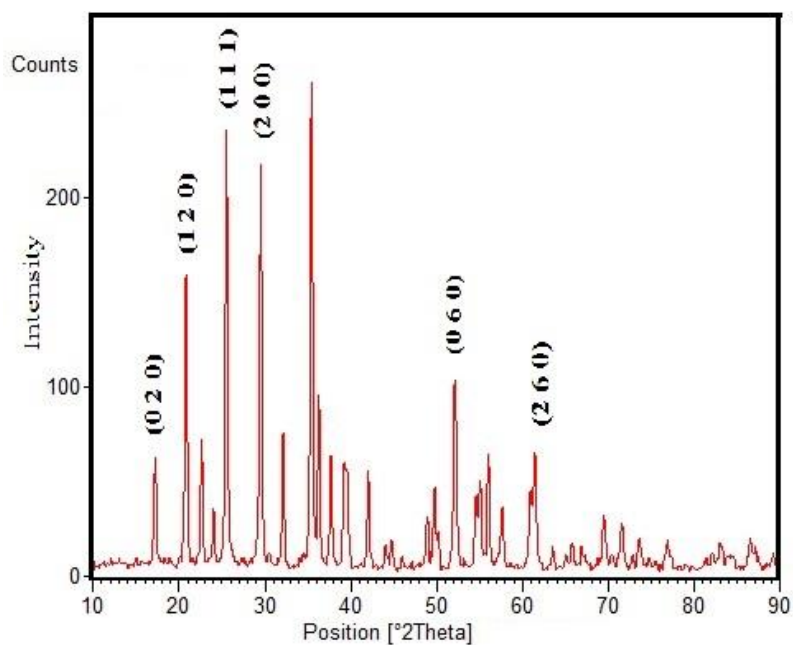


Fig 4.2 XRD result of  $\text{LiMn}_{0.99}\text{Mg}_{0.01}\text{PO}_4$  prepared using 300 $^{\circ}\text{C}$  and 600 $^{\circ}\text{C}$  for 12 hrs effective by solid state reaction method

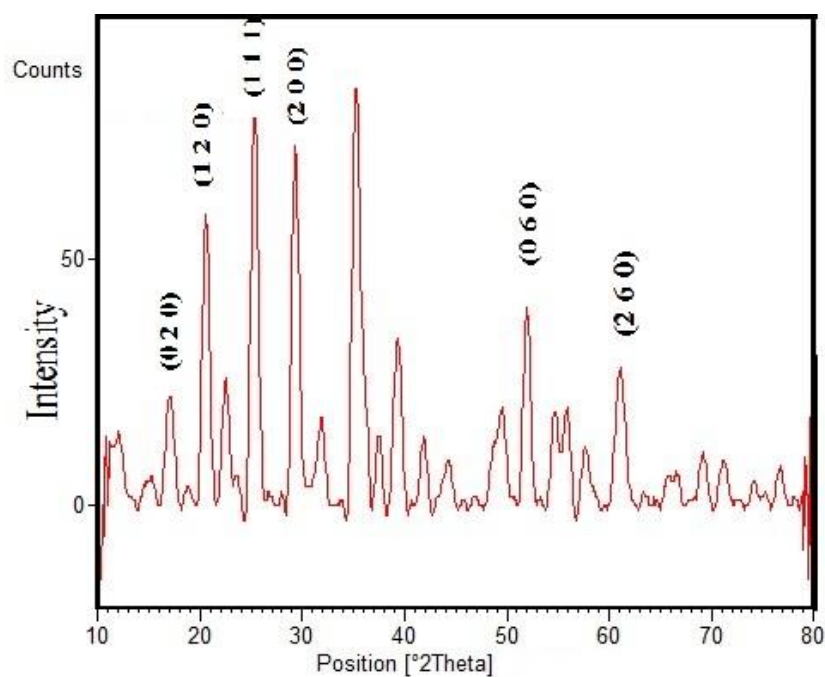
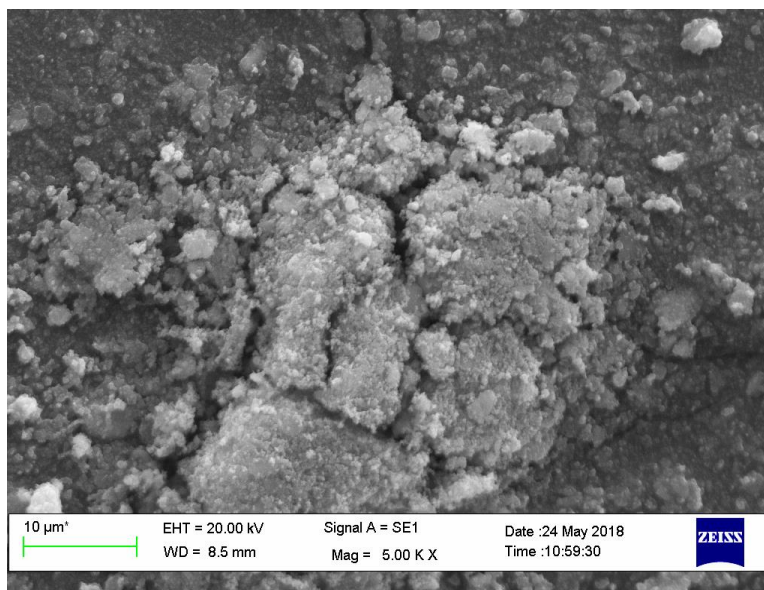


Fig 4.3 XRD result of  $\text{LiMn}_{0.97}\text{Mg}_{0.03}\text{PO}_4$  prepared using 300 $^{\circ}\text{C}$  and 600 $^{\circ}\text{C}$  for 12 hrs effective by solid state reaction method

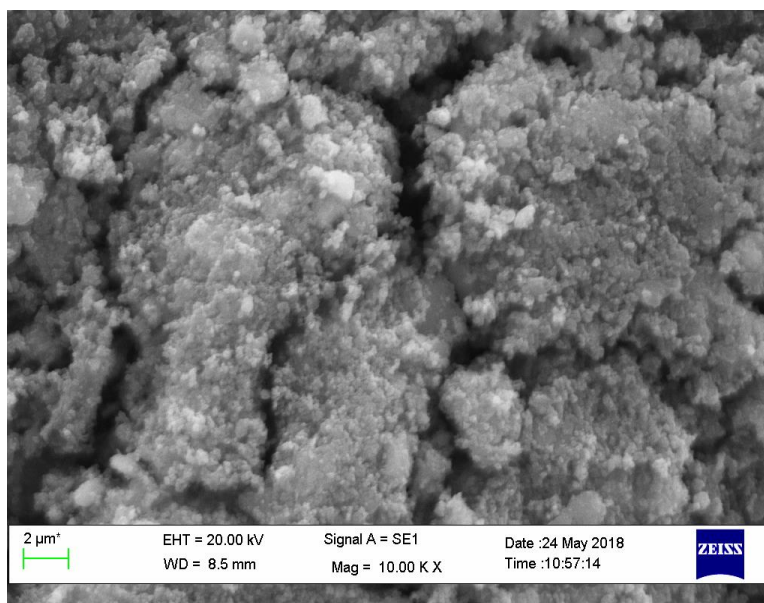
#### 4.1.2 SCANNING ELECTRON MICROSCOPY (SEM):

In Scanning electron microscopy (SEM), electrons used are emitted from the hot filament. Sometimes, Cold cathodes are also used in which a cathode that emits electrons without heating filaments. A very high voltage is used in cold cathode for the emission of electrons which is also known as field emitter. These SEMs are called FE-SEM which gives better images than hot filament SEM. In SEM, backscattered electrons or secondary electrons are detected. Images produced by the backscattered electrons have poorer resolution as compared to the images formed due to secondary electrons, since the energy is emitted from much deeper inside the sample. In SEM, the electron beam is focused on a very small spot size through electrostatic or magnetic lenses. Generally electrostatic lenses are used in SEM. The fine beam is rastered over the sample surface and hence the backscattered electrons are collected by the detector. The image of the sample is generated by the signal from the scan generator along with the amplified signal from the electron collector. In order to protect the filament from oxidation and contamination as well as to reduce the collision between the electrons and air molecules, sample and the filament needs to be kept inside a vacuum chamber. Generally vacuum of  $10^{-2} - 10^{-3}$  Pa is necessary for the normal operation of SEM. However, some manufacturers have developed SEM called environment microscope, where the sample are under high pressure of 100-500 Pa.

Here as-synthesized bare  $\text{LiMnPO}_4$ ,  $\text{LiMn}_{0.99}\text{Mg}_{0.01}\text{PO}_4$  and  $\text{LiMn}_{0.97}\text{Mg}_{0.03}\text{PO}_4$  shows spherical morphology along with the slight agglomeration in the particle of the prepared sample. It also shows the sample thus produced have particles of non-uniform size distribution. The  $\text{LiMnPO}_4$  material consists of particles which have many grains of submicrons which agglomerates to 2-10 $\mu\text{m}$ . The samples are dominated by fine particles of average size 2-10 $\mu\text{m}$ , which are the fragments of large particles. Carbon network connects several nano-sized  $\text{LiMnPO}_4$  which ultimately makes the larger particles. The formation of large  $\text{LiMnPO}_4$  secondary particles would help the electrons and ions transport inside  $\text{LiMnPO}_4$  material.



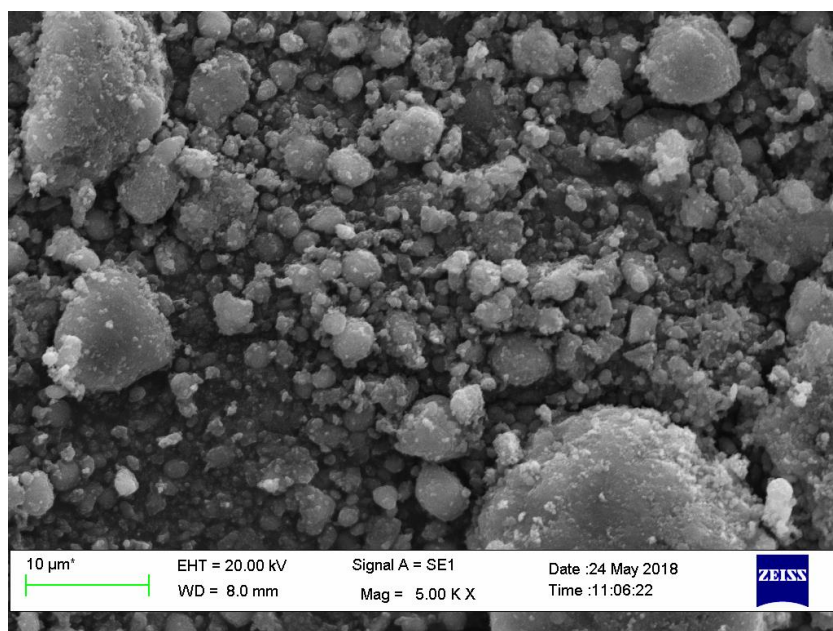
(a)



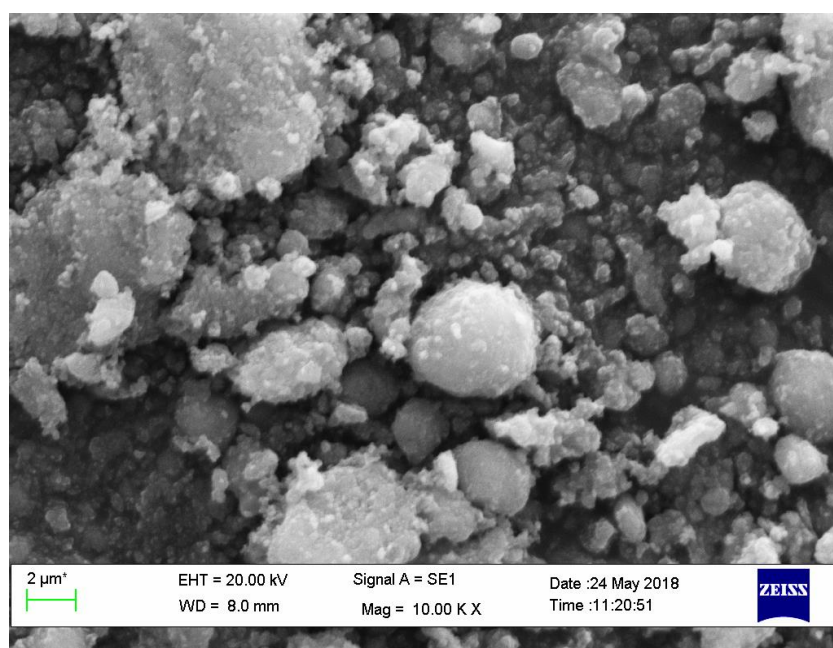
(b)

Fig 4.4 SEM images of  $\text{LiMnPO}_4$  at(a): 5x and (b): 10x zoom





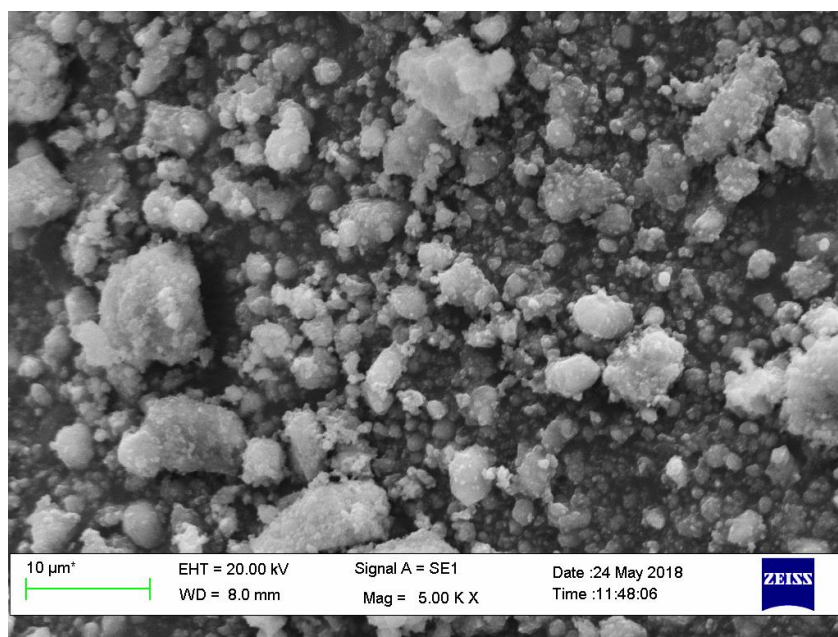
(a)



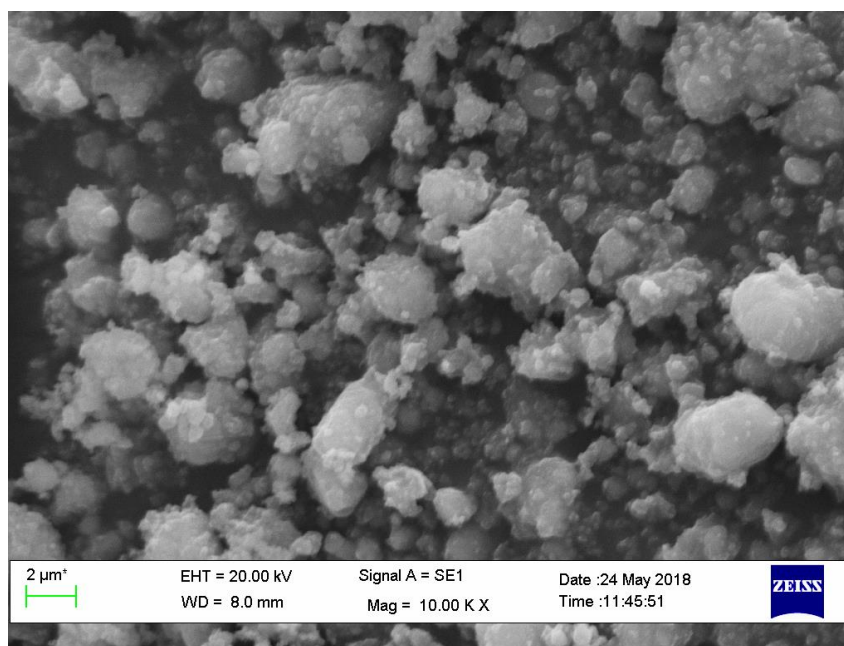
(b)

Fig 4.5 SEM images of  $\text{LiMn}_{0.99}\text{Mg}_{0.01}\text{PO}_4$  at (a): 5x and (b): 10x zoom





(a)



(b)

Fig 4.6 SEM images of  $\text{LiMn}_{0.97}\text{Mg}_{0.03}\text{PO}_4$  at (a): 5x and (b): 10x zoom

#### 4.1.3 ENERGY DISPERSIVE SPECTROSCOPY (EDS):

Scanning electron microscopy is also equipped Energy dispersive spectroscopy which is used for obtaining the compositional details of the sample. The characteristics X-rays interact with the sample which is produced by the high energy. The energy and intensities of the characteristics X- Ray are compared with one another for finding compositional details of the sample under analysis.

The EDS results of the  $\text{LiMnPO}_4$  depicts the composition of the  $\text{LiMnPO}_4$ , which are mainly Mn (36.32% wt.), P(22.79% wt.), O(39.78% wt.) and impurity of Fe (0.01% wt.).

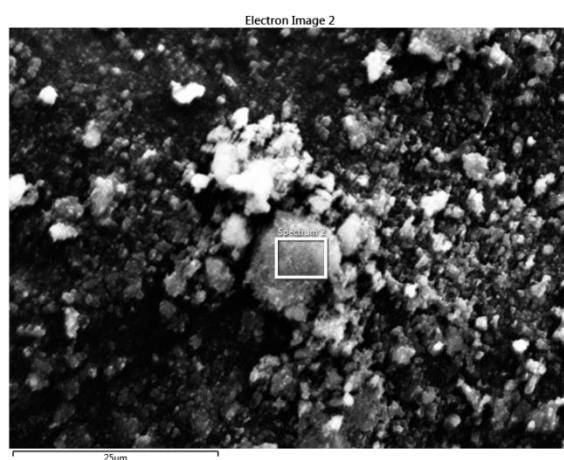


Fig 4.7 EDS image of  $\text{LiMnPO}_4$

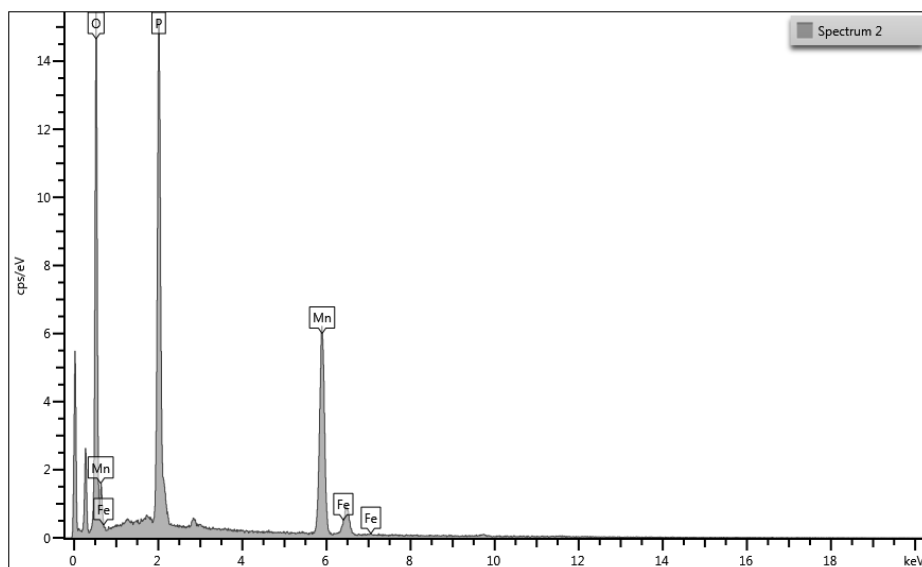


Fig 4.8 Composition of  $\text{LiMnPO}_4$

The EDS results of  $\text{LiMn}_{0.99}\text{Mg}_{0.01}\text{PO}_4$  depicts the composition of  $\text{LiMn}_{0.99}\text{Mg}_{0.01}\text{PO}_4$ , which mainly consists of O(35.86% wt.), Mg(1.10% wt.), P(24.42% wt.) and Mn(39.68% wt.)

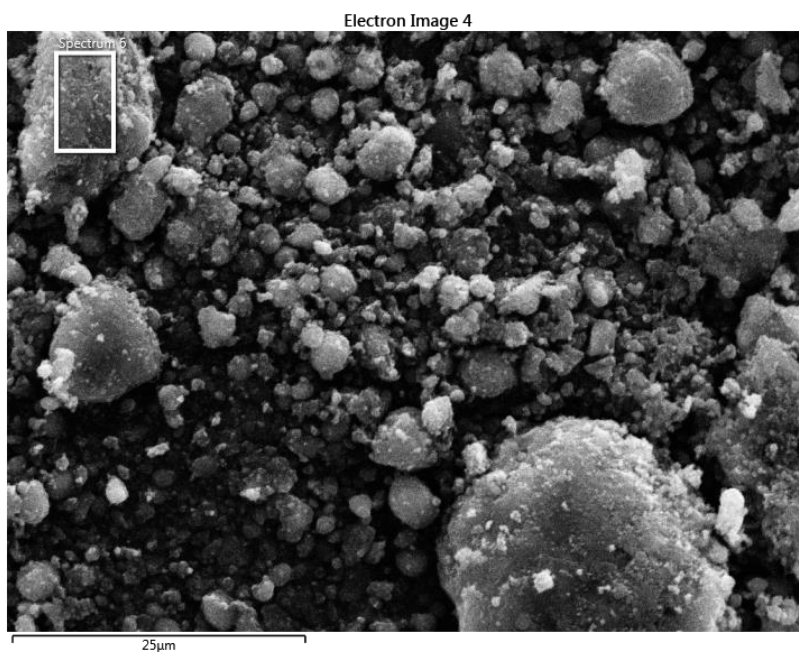


Fig 4.9 EDS image of  $\text{LiMn}_{0.99}\text{Mg}_{0.01}\text{PO}_4$

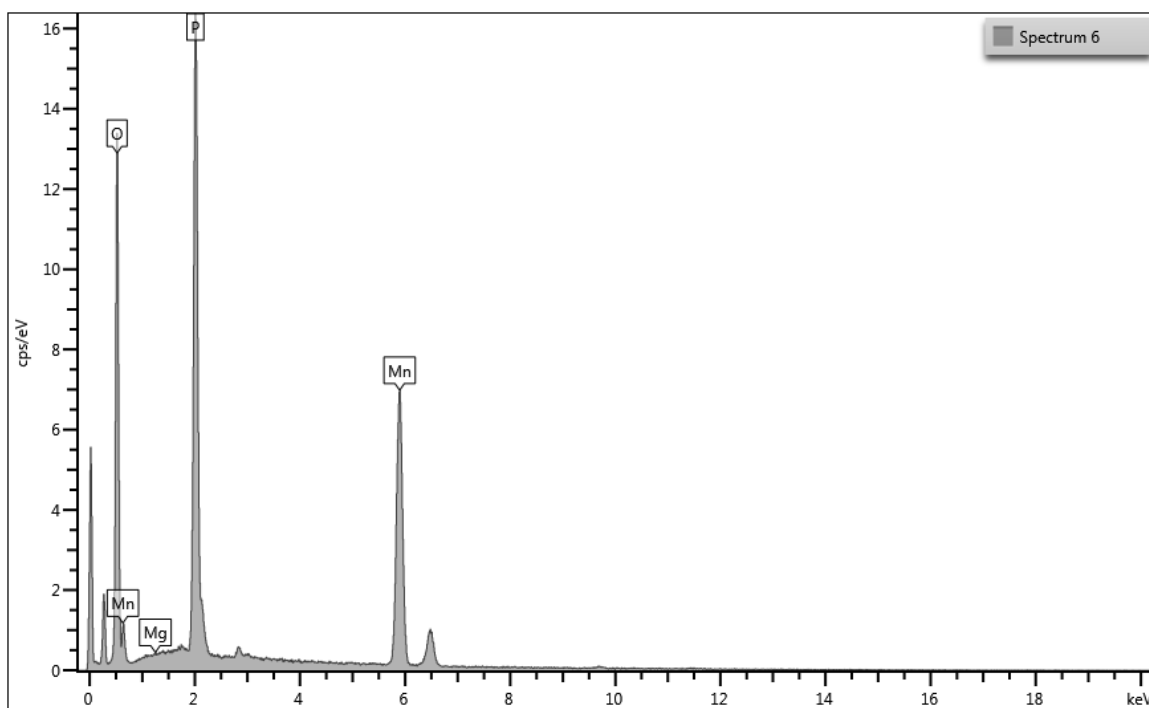


Fig 4.10 Composition of  $\text{LiMn}_{0.99}\text{Mg}_{0.01}\text{PO}_4$

The EDS results of  $\text{LiMn}_{0.97}\text{Mg}_{0.03}\text{PO}_4$  depicts the composition of  $\text{LiMn}_{0.97}\text{Mg}_{0.03}\text{PO}_4$ , which mainly consists of O(43.23% wt.), Mg(3.2% wt.), P(22.07% wt.) and Mn(33.94% wt.)

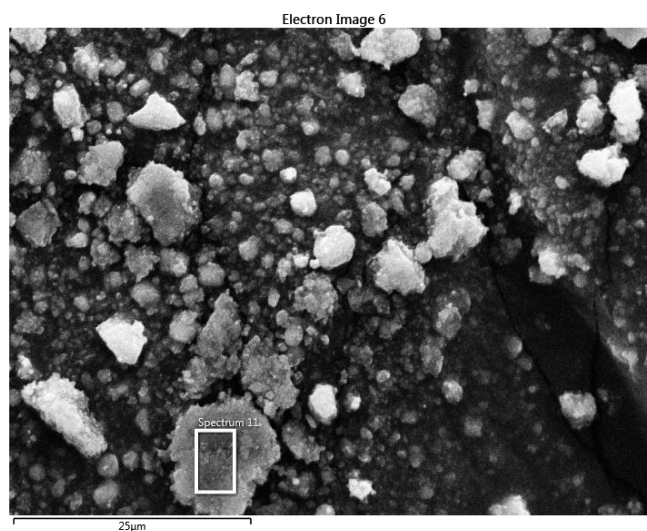


Fig 4.11 EDS image of  $\text{LiMn}_{0.97}\text{Mg}_{0.03}\text{PO}_4$

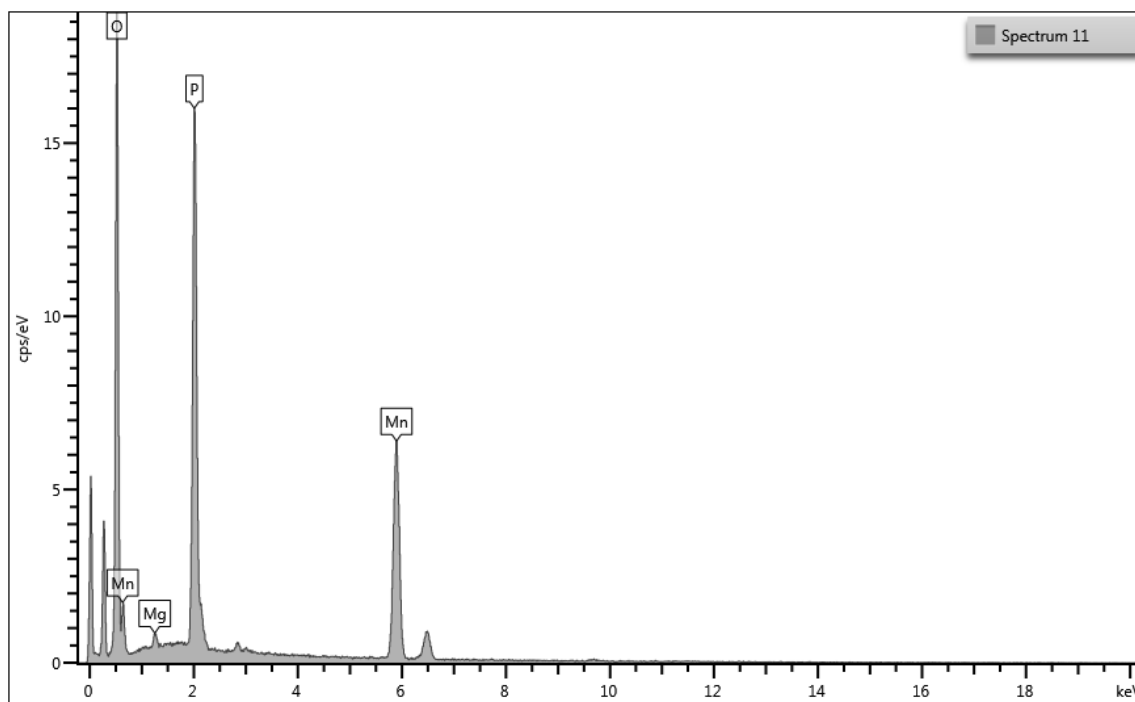


Fig 4.12 Composition of  $\text{LiMn}_{0.97}\text{Mg}_{0.03}\text{PO}_4$

## 4.2 ELECTROCHEMICAL ANALYSIS:

In order to evaluate the electrochemical analysis, cathode were synthesized using the powder by mixing 80 wt.% active powder, that is  $\text{LiMnPO}_4$  (LMP),  $\text{LiMn}_{0.99}\text{Mg}_{0.01}\text{PO}_4$  (LMMP1),  $\text{LiMn}_{0.97}\text{Mg}_{0.03}\text{PO}_4$  (LMMP3), 5 wt.% carbon black and 15 wt.% polyvinylidene fluoride (PVDF). The slurries thus were spread on Aluminium foil. After coating, the cathode were pressed and dried at  $60^\circ\text{C}$  under vacuum for 24 h. For the counter electrode that is anode, Li metal was used.  $\text{LiPF}_6$  was used as the electrolyte and separator used for the cell was Celgard 2400. Argon filled glove box was utilized for the assembly of half cell.

## CHAPTER-5

### CONCLUSION

#### 5.1 CONCLUSION:

Mg<sup>2+</sup> doped LiMnPO<sub>4</sub>/C has been synthesized via a solid-state reaction. In order to overcome the low conductivity of the LiMnPO<sub>4</sub> cathode material, the LiMnPO<sub>4</sub> doped with Mg. The results of XRD and EDS confirm the orthorhombic olivine structure of LiMnPO<sub>4</sub>, LiMn<sub>0.99</sub>Mg<sub>0.01</sub>PO<sub>4</sub> and LiMn<sub>0.97</sub>Mg<sub>0.03</sub>PO<sub>4</sub>. The XRD results confirmed that there was impurity peak detected. It has orthorhombic olivine structure with the space group Pnmb. It can also be confirmed from SEM observations that the final samples were the LiMnPO<sub>4</sub>/C and Mg doped LiMnPO<sub>4</sub> nanocomposites with approximately 2-10  $\mu$ m in primary particles size. A new LiMnPO<sub>4</sub>, LiMn<sub>0.99</sub>Mg<sub>0.01</sub>PO<sub>4</sub> and LiMn<sub>0.97</sub>Mg<sub>0.03</sub>PO<sub>4</sub> thus prepared with Mg doped proposed to enhance the electrochemical performance of the LiMnPO<sub>4</sub> material, it is necessary to improve both ion and electron transport. The new material thus formed is of high performance cathode material for lithium ion batteries. Although the samples obtained is of larger particle size as compared to the other technologies but still it is less toxic, environment friendly and low cost cathode material. The doping in the cathode material shows the positive effect. We have synthesized highly regular LiMnPO<sub>4</sub> and Mg doped LiMnPO<sub>4</sub>, 1% wt. and 3% wt., which facilitates electron transfer and Li<sup>+</sup> transport. Compared with LiMnPO<sub>4</sub>/C sample, Mg doped LiMnPO<sub>4</sub>/C composites display larger lithium ion diffusion coefficient.

## REFERENCES

- [1] **Nonaqueous synthesis of nano-sized  $\text{LiMnPO}_4/\text{C}$  as a cathode material for high performance lithium ion batteries** -Year-2016- Jingmin fan, Yang Yu, yang Wang, Qi-Hui Wu, Mingsen Zheng, Quanfeng Dong, State key Lab of Physical Chemistry of solid surfaces, Dept of Chemistry, College of chemistry and Chemical Engineering, Xiamen University, China, Dept of Chemistry, College of Chemistry and Life Science, Quanzhou Normal university, China
- [2] **Improved electrochemical activity of  $\text{LiMnPO}_4$  by high-energy ball milling-Year 2011-** Jiangfeng Ni, Yoshiteru Kawabe, Masanori Morishita, Masaharu Watada, Tetsuo Sakai, National Institute of Advanced industrial Science and Technology, japan, GS Yuasa International Ltd, Japan
- [3] **Improving the Electrochemical performance of  $\text{LiMnPO}_4/\text{C}$  by liquid nitrogen Quenching** - Year-2013 – Ling Wu, Shengkui Zhong, Fan Lv, Jiequn Liu, School of Iron and Steel, Soochow University, Suzhou 215000, PR China
- [4]  **$\text{LiMnPO}_4$  nanoplates grown via a facile surfactant-mediated solvothermal reaction for high-performance Li-ion batteries** - Year-2014 – Wenxuan Zhang, Zhongqiang Shan, Xiaoyan Liu, School of Chemical Engineering and Technology, Tianjin University, PR China
- [5] **Synthesis and electrochemical performance of Ti-Fe co-doped  $\text{LiMnPO}_4/\text{C}$  as cathode material for lithium-ion batteries - Year 2016-** Qiao-Ying Huang, Zhi Wu, Jing Su, Yun-Fei Long, Xiao-yan Lv, Yan Xuan Wen, School of Chemistry and Chemical Engineering, Guangxi University, PR China, Guangxi colleges and universities key laboratory of Novel Energy Materials and Related Technology, PR China, The New Rural Development Research Institute, Guangxi University, China
- [6] **Effect of particle size on  $\text{LiMnPO}_4$ - Year 2007-** Thierry Drezen, Nam-Hee Kwon, Paul Bowen, Ivo Teerlinck, Motoshi Isono, Ivan Exnar, High Power Lithium, Swiss Federal Institute

of technology, Lausanne, Switzerland, Material Engineering Division, Toyota Motor corporation, Japan

**[7] Li-ion battery materials: present and future** – Year 2015 - Naoki Nitta, Feixiang Wu, Jung Tae Lee and Gleb Yushin, School of Materials Science and Engineering, Georgia Institute of Technology, Atlanta, GA, USA, School of Metallurgy and Environment, Central South University, Changsha, China.

**[8]  $\text{LiMn}_{0.8}\text{Fe}_{0.19}\text{Mg}_{0.01}\text{PO}_4/\text{C}$  as a high performance cathode material for lithium ion batteries** – Year 2011- Haisheng Fang, Enrui Dai, Bin Yang, Yaochun Yao, , Wenhui Ma, Faculty of Metallurgical and Energy Engineering, Kunming University of Science and Technology, Kunming, China, National Engineering Laboratory for Vacuum Metallurgy, Kunming University of Science and Technology, Kunming, China, Key Laboratory of Nonferrous Metals Vacuum Metallurgy of Yunnan Province, Kunming University of Science and Technology, Kunming, China.

**[9] Effect of Zn doping on the performance of  $\text{LiMnPO}_4$  cathode for lithium ion batteries** – Year 2012- Haisheng Fang, Huihua Yi, Chenglin Hu, Bin Yang, Yaochun Yao, Wenhui Ma, Yongnian Dai, Faculty of Metallurgical and Energy Engineering, Kunming University of Science and Technology, Kunming, China, National Engineering Laboratory for Vacuum Metallurgy, Kunming University of Science and Technology, Kunming, China, Key Laboratory of Nonferrous Metals Vacuum Metallurgy of Yunnan Province, Kunming University of Science and Technology, Kunming, China

**[10] Enhanced electrochemical performance of nano  $\text{LiMnPO}_4$  with multifunctional surface co-coating of  $\text{Li}_2\text{TiO}_3$  and carbon**-Year-2015- Zhijian Zhang, Guorong Hu, Yanbing Cao, Jainguo Duan, ke Du, Zhongdong Peng, School of Metallurgy and Environment, Central South University, China.

**[11] Physical and electrochemical properties of  $\text{LiMnPO}_4/\text{C}$  composite cathode prepared with different conductive carbons**- year 2010- Zhumabay Bakenov, Izumi Taniguchi, Department of chemical Engineering, Tokyo Institute of Technology, Tokyo, Japan



**[12] Cathode performance of  $\text{LiMnPO}_4/\text{C}$  nanocomposites prepared by combination of spray pyrolysis and wet ball-milling followed by heat treatment-** Year 2010- The Nam Long Doan, Izumi Taniguchi, dept of Chemical Engineering, Graduate School of Science and Engineering, Tokyo Institute of Technology, Japan

**[13] Comparative study of  $\text{LiMnPO}_4/\text{C}$  cathodes synthesized by polyol and solid-state reaction methods for Li-ion batteries** – Year 2012 - Nicholas P.W. Pieczonka, Zhongyi Liu, Ashfia Huq, Jung-Hyun Kim, Chemical & Materials Systems Laboratory, General Motors Global R&D Center, Warren, USA, Electrochemical Energy Research Laboratory, General Motors Global R&D Center, Warren, USA, d Neutron Scattering Science Division, Oak Ridge National Laboratory, Oak Ridge, USA

**[14] Synthesis of  $\text{LiMnPO}_4/\text{C}$  composite material for lithium ion batteries by sol-gel method-** year 2012- Zhong Sheng-Kui, Wang You, Liu Jie-qun, Wang Jian, GuangXi Key Laboratory of New energy and Building Energy saving, Guilin University of technology, China, College of Chemistry and Bioengineering, Guilin Univeristy of technology, Guilin, China, Shagang school of iron and steel , Soochow university, China

**[15] Mesoporous  $\text{LiMnPO}_4/\text{C}$  nanoparticles as high performance cathode material for lithium ion batteries** – Year 2016 - Fang Wen, Hongbo Shu, Yuanyuan Zhang, Jiajia Wan, Weihua Huang, Xiukang Yang, Ruizhi Yu, Li Liu, Xianyou Wang, Key Laboratory of Environmentally Friendly Chemistry and Applications of Ministry of Education, School of Chemistry, Xiangtan University, Hunan, Xiangtan, China

**[16] Utilizing active multiple dopants (Co and Ni) in olivine  $\text{LiMnPO}_4$**  – Year 2012 - Manickam Minakshi, Sathiyaraj Kandhasamy, Faculty of Minerals and Energy, Murdoch University, Murdoch, Australia

**[17]  $\text{LiMnPO}_4$ : Review on Synthesis and Electrochemical Properties** – Year 2015 - Joel O. Herrera, Héctor Camacho-Montes, Luis E. Fuentes, Lorena Álvarez-Contreras, Universidad Autónoma de Ciudad Juárez, Cd. Juárez, México, Centro de Investigación en Materiales Avanzados, Chihuahua, México

**[18] Ionothermal synthesis and electrochemical analysis of Fe doped LiMnPO<sub>4</sub>/C composites as cathode materials for lithium-ion batteries** –Year 2014- Xueliang Li, Shuai Liu, Hongchang Jin, Yu Meng, Yunfu Liu, School Of Chemical Engineering, hefei University, China, Anhui Key Laboratory of controllable chemical Reaction and material chemical Engineering, China